LBL-11212
Preprint

Lawrence Berkeley Laboratory
UNIVERSITY OF CALIFORNIA

EARTH SCIENCES DIVISION

Submitted to Journal of Geophysical Research

INTERPRETATION OF SHALLOW ELECTRICAL FEATURES FROM ELECTROMAGNETIC AND MAGNETOTELLURIC SURVEYS AT MOUNT HOOD, OREGON

N.E. Goldstein, E. Mozley, and M. Wilt

April 1981

Prepared for the U.S. Department of Energy under Contract W-7405-ENG-48

LBL-11212

INTERPRETATION OF SHALLOW ELECTRICAL FEATURES FROM ELECTROMAGNETIC AND MAGNETOTELLURIC SURVEYS AT MOUNT HOOD, OREGON

N. E. Goldstein, E. Mozley,* and M. Wilt

Earth Sciences Division
Lawrence Berkeley Laboratory
University of California
Berkeley, California 94720

*Materials Sciences and Mineral Engineering
College of Engineering
University of California
Berkeley, California 94720

April 1981

This work was supported by the Assistant Secretary for Conservation and Renewable Energy, Office of Renewable Technology, Division of Geothermal and Hydropower Technologies of the U.S. Department of Energy under Contract No. W-7405-ENG-48.

ABSTRACT

A magnetotelluric survey, with a reference magnetometer for noise cancellation, was conducted at accessible locations around Mt. Hood, Oregon. Thirty-eight tensor magnetotelluric (MT) and remote telluric stations were set up in clusters around the volcano, except for the northwest quadrant, a wilderness area. Because of limited access, station locations were restricted to elevations below 1829 m, or no closer than 5 km from the 3,424-m summit. On the basis of the MT results, three areas were later investigated in more detail using a large-moment, controlled-source electromagnetic (EM) system developed at Lawrence Berkeley Laboratory (LBL) and the University of California at Berkeley. One-dimensional interpretations of EM and MT data on the northeast flank of the mountain near the Cloud Cap eruptive center and on the south flank near Timberline Lodge show a similar subsurface resistivity pattern: a resistive surface layer 400-700 m thick, underlain by a conductive layer with variable thickness and resistivity of < 20 ohm·m. It is speculated that the surface layer consists of volcanics partially saturated with cold meteoric water. The underlying conductive zone is presumed to be volcanics saturated with water heated within the region of the central conduit and, possibly, at the Cloud Cap side vent. This hypothesis is supported by the existence of warm springs at the base of the mountain, most notably Swim Warm Springs on the south flank, and by several geothermal test wells, one of which penetrates the conductor south of Timberline Lodge. The MT data typically gave a shallower depth to the conductive zone than did the EM data. This is attributed, in part, to the error inherent in one-dimensional MT interpretations of geologically or topographically complex areas. On the other hand, MT was better for resolving the thickness of the conductive layer and deeper structure. The MT

data show evidence for a moderately conductive north-south structure on the south flank below the Timberline Lodge and for a broad zone of late Tertiary intrusives concealed on the southeast flank.

INTRODUCTION

As part of a geothermal energy assessment of Mt. Hood, Oregon, the U.S. Department of Energy (DOE), the U.S. Geological Survey, the U.S. Forest Service, and the State of Oregon's Department of Geology and Mineral Industries have undertaken a series of geological, geochemical, and geophysical studies around this Holocene stratovolcano located 100 km east of Portland, Oregon (Figure 1). Under contract to the U.S. Department of Energy's Division of Geothermal Energy, Lawrence Berkeley Laboratory was responsible for geochemical and electrical resistivity surveys (Goldstein et al., 1978; Goldstein and Mozley, 1978; Wilt et al., 1979; and Wollenberg et al., 1979). These and other studies were conducted to obtain basic information on the geothermal potential of the area.

Because of the rugged terrain, a general lack of access roads around Mt. Hood, and high contact resistance, we concluded early that conventional dc resistivity surveys would be impractical for deep exploration. We therefore embarked on a program of magnetotellurics with a reference magnetometer for noise cancellation and satellite telluric stations (Goldstein and Mozley, 1978). This work, done under contract by Geonomics, Inc., was followed by a controlled-source electromagnetic sounding program in 1978 using the large-moment, EM-60 system (Morrison et al., 1978), developed at LBL and the University of California at Berkeley.

In this paper, we discuss the results of these surveys, comparing the MT and EM interpretations and examining the usefulness of these techniques for geothermal prospecting at a High Cascade volcano.

GEOLOGICAL SETTING

Mt. Hood is one of several major Pleistocene composite andesitic volcanoes in a chain extending from northern California to British Columbia (Figure 1). Volcanism along this belt is believed by many to result from the eastward subduction of the Juan de Fuca plate beneath the North American plate.

Mt. Hood rises some 2500 m above the platform of upper Miocene Columbia River basalts (CRB) and younger Pliocene volcanics consisting of andesitic plugs and flows (Figure 2). Development of the main body of the cone was completed about 20,000 years ago (Wise, 1968), and renewed volcanism has occurred at various times since. Several domes were extruded near the summit about 12,000 years ago (Crandell and Rubin, 1977), and later episodes of volcanism caused collapse of the south rim of the crater roughly 1600 years ago. Minor eruptions are reported to have occurred as recently as 1859 and 1865 (Folsom, 1970).

Present-day thermal manifestations are warm water springs (Swim Warm Springs) near Summit Meadows on the south flank, and a number of fumaroles in the summit area around Crater Rock, a hornblende dacite plug extruded 200 to 300 years ago (Crandell, 1980).

The predominant surficial material covering Mt. Hood is andesitic clastic debris. The extensive lava flows predating the debris are mainly hornblende andesite; the more recent extrusions from satellite vents on the north and northeast flanks of the volcano are olivine basalt and olivine andesite. Glacial deposits from the Fraser glaciation period (8000 to 15,000 years ago) and recent mudflows and alluvium fill many of the valleys.

Little substantiated structural information was available when we began

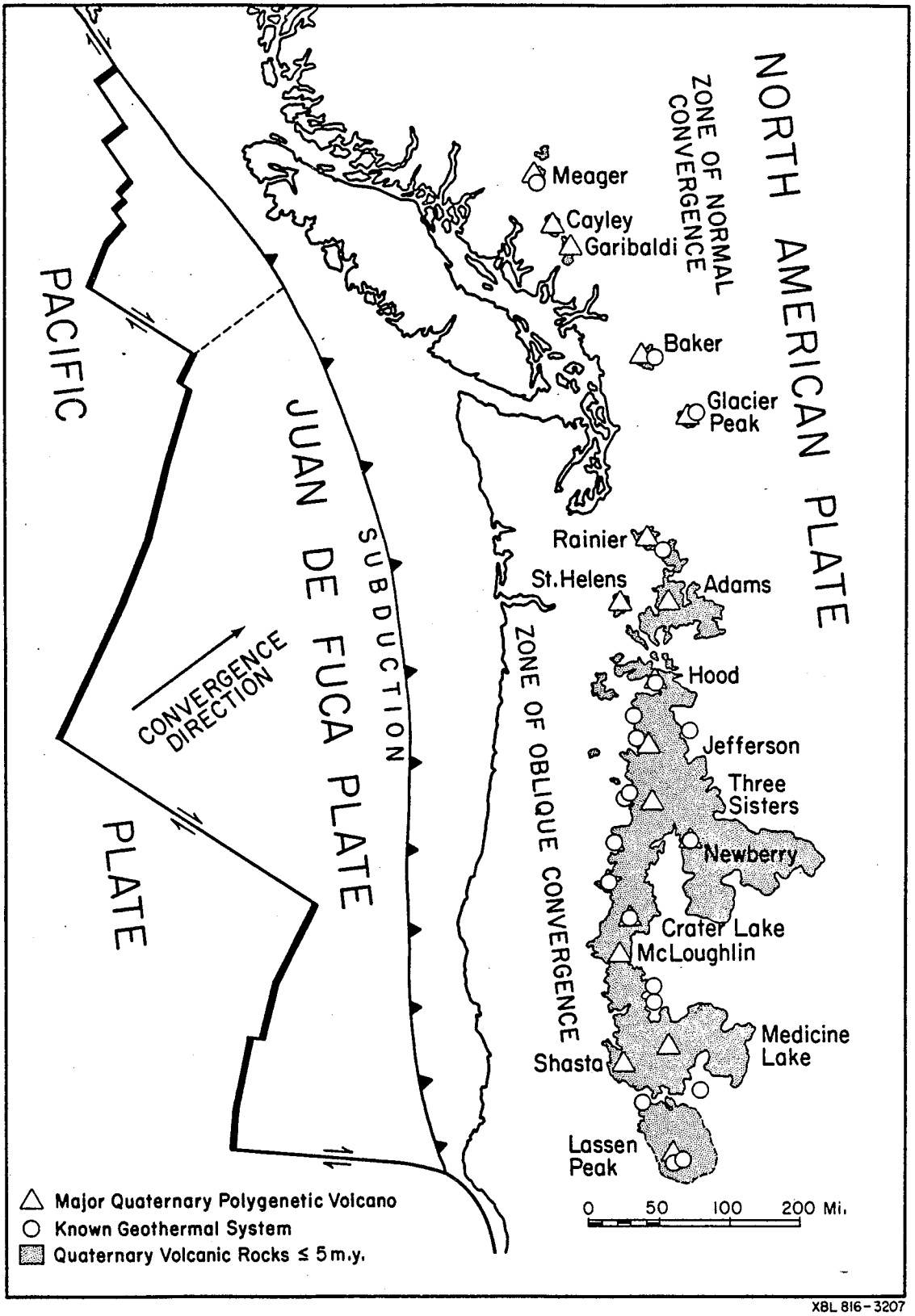

Figure 1. Location of volcanoes and Holocene volcanic rocks of the Cascade Range (after Bacon, 1981).

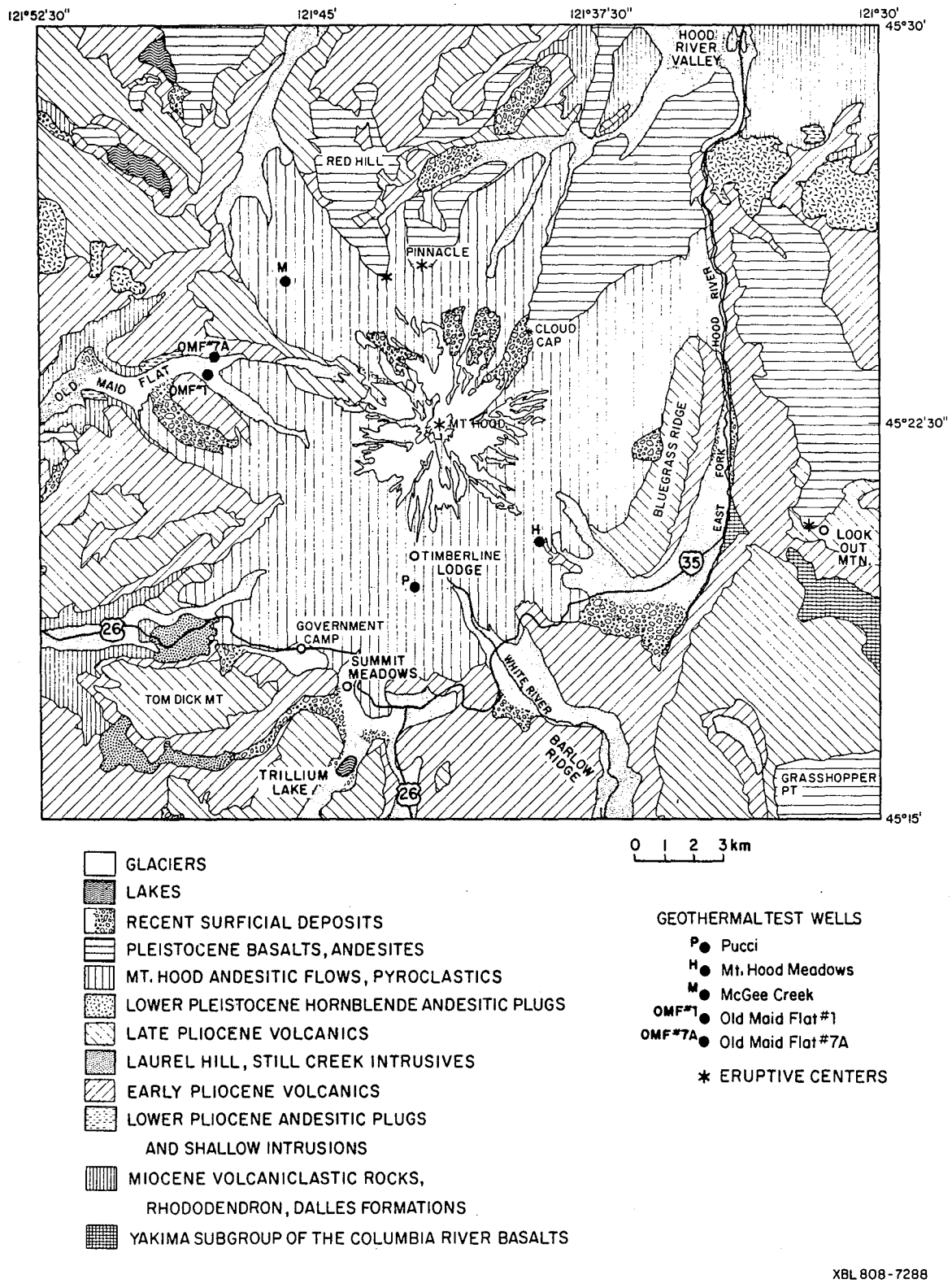

Figure 2. A simplified geological map of the Mt. Hood area (after Wise, 1968).

the geophysical surveys. Allen (1966) stated that Mt. Hood lies within a graben formed by the north-south Hood River-Green Ridge faults (along the East Fork of the Hood River) on the east and by unnamed faults recognized by Thayer (1937) and Callaghan (1933) on the west. On the basis of their gravity survey, Couch and Gemperle (1979) concluded that Mt. Hood is superimposed on a gravity low that could be a north-south graben-like structure.

Recently, Beeson and Moran (1979) provided new information on a stratigraphic-structural model for the pre-Mt. Hood volcanics. They found evidence that the CRB underlying Mt. Hood may total 500 m in thickness and have been gently folded into asymmetrical anticlines and synclines striking N 40° to 65° E. Some anticlines are thrust-faulted on the northwest limb with thrusting SE to NW. Superimposed on this is a system of NNW-trending fractures and faults. Some faults display slickensides indicating right-lateral movement. The CRB dip gently away from the axis of the High Cascades near Mt. Hood, forming a broad structural high that Beeson and Moran (1979) postulate to be a consequence of crustal swelling caused by intrusion.

Before this study there were few reported electrical studies of the crust beneath the Cascades, and no studies specific to any one of the Quaternary volcanoes. Law et al. (1980) made deep geomagnetic depth soundings at six stations in an east-west line crossing the Cascades 120 km north of Mt. Hood--the line passing between Mt. Rainier and Mt. St. Helens. They found evidence for a north-south conductivity anomaly close to the axis of the High Cascades, and they fitted the anomaly to a line current at a depth of 17 km. Because of nonuniqueness, the source might also correspond to a current system up to 50 km wide located at a shallower depth. They also found evidence in the quadrature component for a near-surface conductor. The U.S. Geological Survey (Stanley, 1980) later contracted for a regional MT survey at widely

spaced lines across the Cascades, with one line at roughly the same latitude as the geomagnetic sounding stations. Because of poor data quality or 3-D effects in the data, no detailed interpretation was done. The MT electrical strike, however, has a N 70° E trend, which Stanley (1980) shows is parallel to the strike of a large gravity low (-100 mGal) crossing the Cascades obliquely between the Columbia River and Mt. Rainier. The MT data indicate a conductor to the south, or toward the gravity low. Thus, from these two limited surveys, one might argue for both a crustal conductor oriented north-south beneath the Cascades and a large, near-surface block of less dense, but relatively conductive, Holocene volcanics north of the Columbia River.

GEOPHYSICAL SURVEY INSTRUMENTATION AND PROCEDURES

Magnetotelluric Surveys

Magnetotelluric surveys were performed in two phases by Geonomics, Inc., from June to November 1977. Each setup consisted of a tensor MT base station plus two remote telluric stations and one remote magnetic station at distances of 2-4 km from the base station (Figure 3). From each remote site, electrical and magnetic field data were telemetered via an FM radio link to the base station, where all data, in three overlapping bands from 0.002 to 40 Hz, were digitized and recorded on magnetic tape. The second three-component SQUID magnetometer was placed at one of the remote stations so that we could later perform reference magnetic MT processing for noise cancellation (Gamble et al., 1979). The other two remote stations consisted of a pair of orthogonal electrical dipoles and associated electronics. These remote telluric stations were used as quasi-tensor MT stations on the assumption that the magnetic field is spatially uniform over the distance between base and remote stations

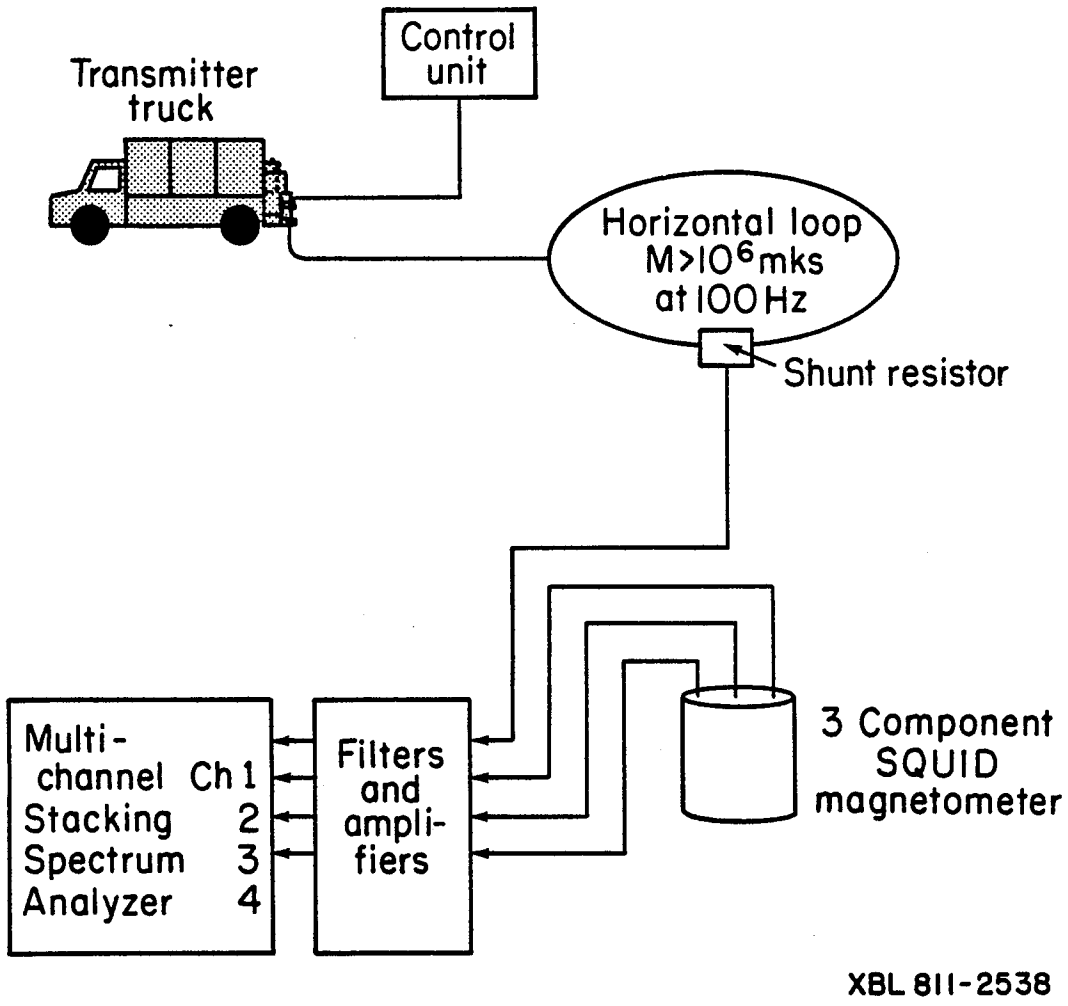

Figure 3. A schematic diagram of the telluric-magnetotelluric data acquisition method with a reference magnetometer.

(Hermance and Thayer, 1976). To check the assumption of magnetic field uniformity, one of the remote telluric stations became the base for the next set of measurements. In other cases, the reference magnetometer was located at a remote telluric station. Both procedures confirmed that the assumption of field uniformity holds.

Following the contractor's conventional data processing, all data were reprocessed by using both the remote magnetic and remote electric fields as reference fields. We found that both references worked well for calculating unbiased impedance estimates, but the impedance estimates calculated using the reference electric signals had larger statistical errors because of greater noise in the electric field.

Electromagnetic Surveys

Figure 4 shows the configuration of the EM-60 system, used for controlled-source EM soundings. A large magnetic moment ($>10^6$ MKS) was created by impressing currents of ±65 A at ±150 V into a square loop consisting of three turns, 100 m on a side, of No. 6 welding cable. The frequency of the applied square-wave current was remotely controlled and could be made to vary discretely between 10^{-3} Hz and 10^3 Hz. For this work, however, we were restricted to the frequency range 0.1-200 Hz because of large geomagnetic and atmospheric noise energy below and above this range, respectively.

At the receiver locations, magnetic field signals were detected by means of a three-component cryogenic (dc SQUID) magnetometer oriented to detect the vertical, radial, and tangential field components. Signals were amplified and band-pass filtered for anti-aliasing and signal-to-noise improvement, then were processed directly by means of a multichannel, microprocessor-controlled spectrum analyzer (Morrison et al., 1978). The spectrum analyzer stacked a

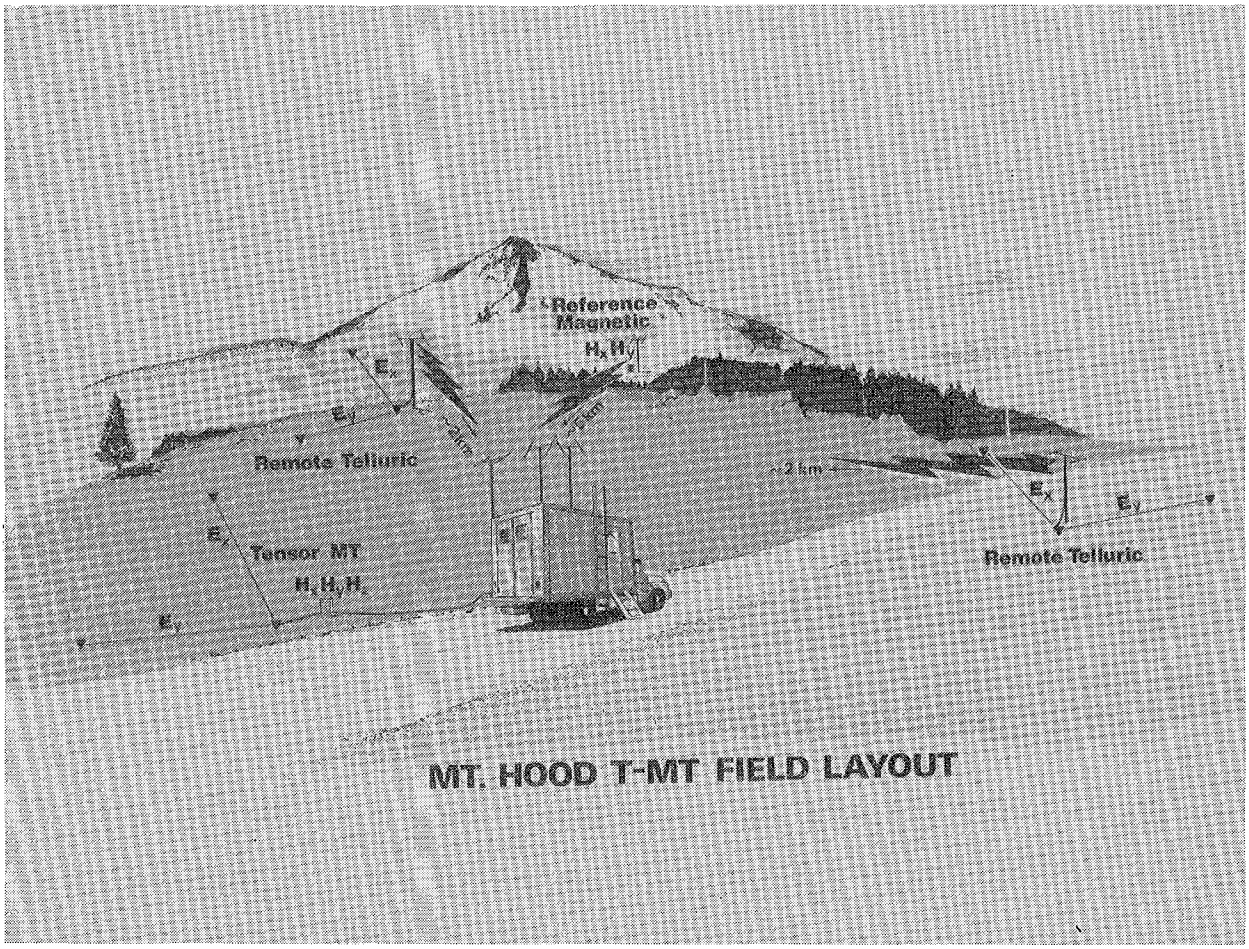

BBC 770-12414

Figure 4. The LBL controlled-source EM system (EM-60).

specified number of cycles and computed and displayed an average "raw" amplitude and phase relative to current phase in the loop. A hard-wire link between the spectrum analyzer and a 0.01 ohm, 0.01% shunt resistor on the loop provided the phase reference. Spectral estimates were made at the fundamental and at higher odd harmonics, up to the seventh, as specified by the operator.

Data interpretation was accomplished by means of a one-dimensional inversion using an automatic Marquardt least-squares approach (e.g., Inman, 1975). The program fits amplitude/phase parameters of the field components normal to the plane of the loop (H_N and ϕ_N), radially outward from the loop (H_R and ϕ_R), and jointly fits polarization ellipse parameters (ellipticity and tilt angle). The tangential field, which should be absent over a layered earth or on a line perpendicular to a two-dimensional structure, was also monitored. Two-dimensional modeling, although possible, was not used for reasons of cost and the small number of stations.

Analysis of the EM data was complicated by the presence of cultural EM noise and sloping terrain. The noise required use of 60-Hz and 180-Hz notch filters whose effect on neighboring frequencies had to be carefully determined. More formidable was the rugged terrain, which resulted in a magnetic dipole vector inclined to the vertical. Because the resulting source is a combination of vertical and horizontal dipoles, it was necessary to correct the observed signals before an interpretation was made. As a first approximation, we mathematically rotated the vertical (H_N) and radial (H_R) components of the observed signals to find the fields normal to and in the plane of the transmitter loop. The criteria used to define these fields are that $H_N \rightarrow H_P$ and $H_R \rightarrow 0$ as $f \rightarrow 0$, where H_P is the calculated primary field at the magnetometer resulting from the transmitter dipole. One other approach successfully tested was to derive the ellipticity of the magnetic

field polarization ellipse, which is independent of loop orientation, and to perform a one-dimensional interpretation on this information alone. Results from the ellipticity analysis compared rather well with results from a joint one-dimensional inversion of H_N and H_R amplitudes and phases. Because the ellipticity approach uses relative phase between H_N and H_R components rather than absolute phase, it also has the advantage of not requiring a phase reference link between transmitter and receiver.

RESULTS

Figure 5 shows the locations of MT base stations, remote telluric stations, and EM-60 transmitter and receiver stations. We concentrated stations in six main areas for various reasons: warm water emanations, geological interest, a nearby end-user of geothermal water, and above all, accessibility.

Cloud Cap

The Cloud Cap area lies on the NE flank of the mountain near a fairly recent (about 12,000 years old) eruptive center. The two MT and three remote telluric stations, all situated in the olivine basalt flow, extend from near the vent (elevation 1820 m) downhill a distance of 3 km (Figure 6). Two EM-60 soundings were made relative to a transmitter loop near the vent.

Using all impedance values of all five MT stations, the best average principal direction of the impedance tensor directions was found to be nearly east-west (S 83° W). The tipper indicated a strike of N 59° W. These results were unexpected, since we had anticipated a northeasterly strike direction, i.e., radially outward from the summit or in the general direction of the successive volcanic flows and main erosional channels. After the average strike direction was determined, the apparent resistivities were

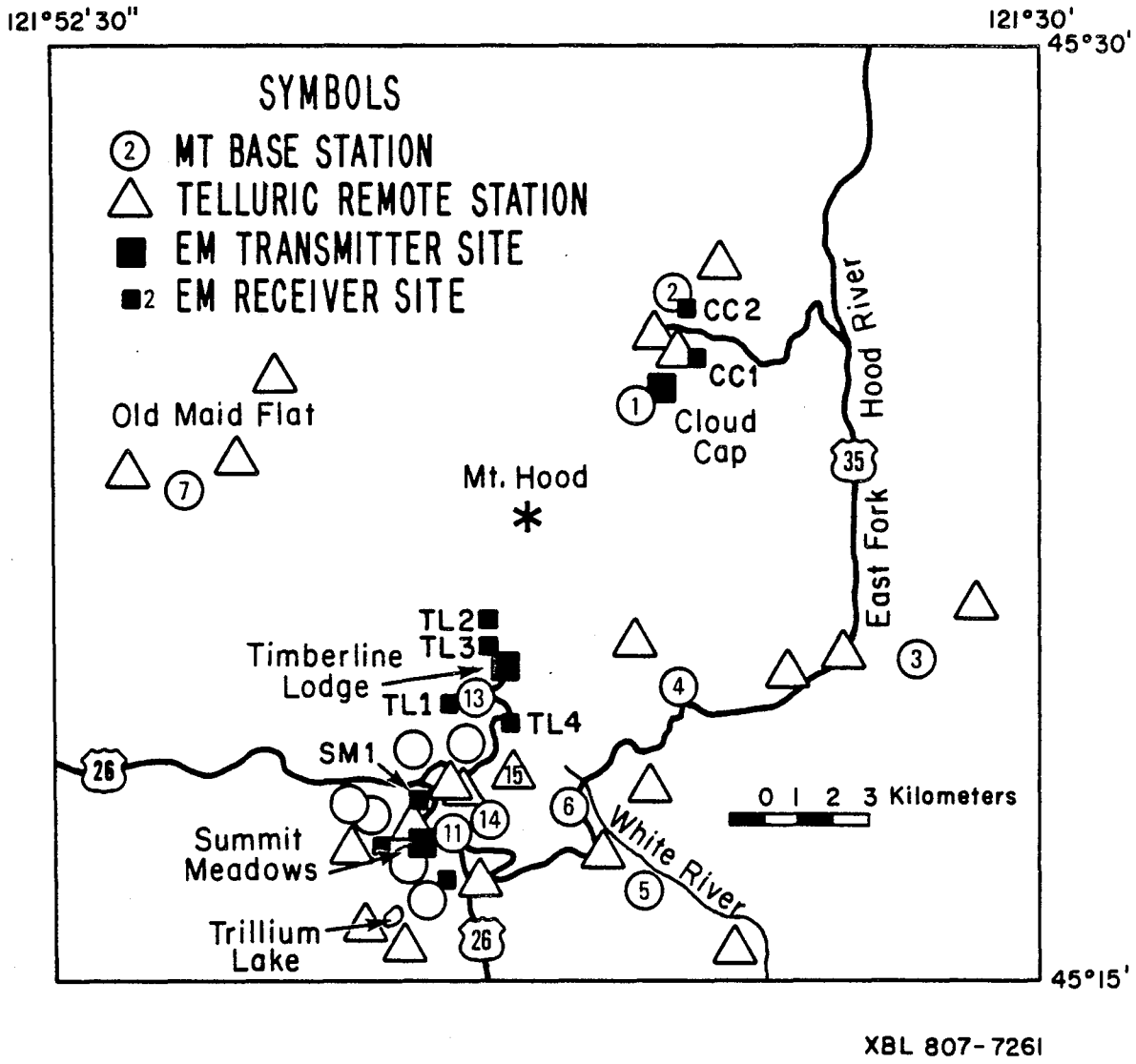

Figure 5. Locations of MT and EM stations. The numbered stations are referred to in the text.

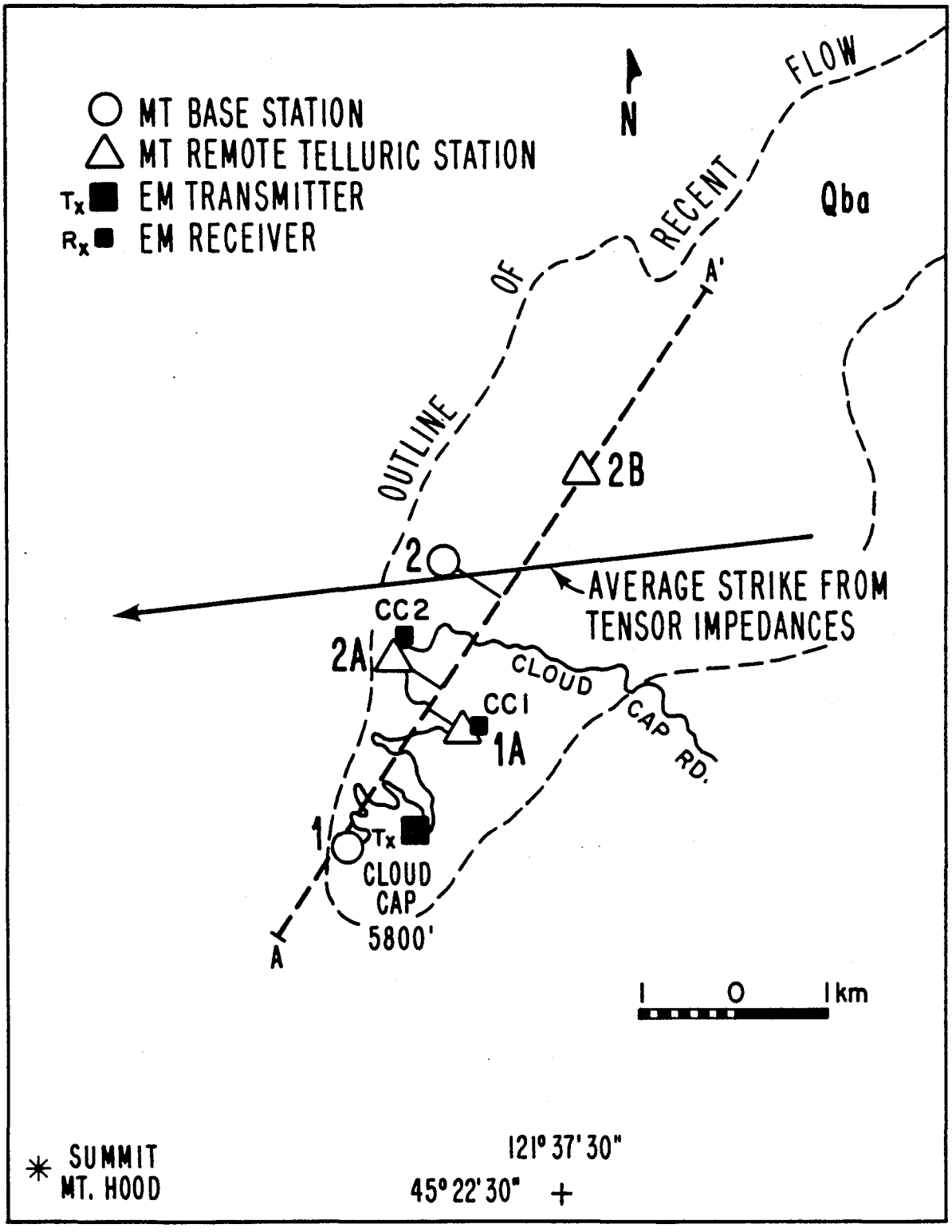

Figure 6. Locations of MT and EM stations in the Cloud Cap area.

calculated from the rotated impedances. These results were fitted to layered models according to a linearized, least-squares inversion modeling scheme (Jupp and Vozoff, 1975), examples of which are shown in Figure 7 for Station 1. The error bars are the 50% confidence limits using χ^2 distribution theory. A one-dimensional interpretation was justified on the basis of the similarity between ρ_{xy} and ρ_{yx} sounding curves, a similarity that exists mainly for the high frequency (i.e., near-surface) regime. Because of the good quality of the high-frequency data at these stations, we overspecified the number of layers and obtained models with a relatively large number of near-surface layers.

In order to obtain a quasi two-dimensional model for the shallow region, we projected the results from all Cloud Cap stations into profile A-A', which is roughly radial to the cone, and obtained the sections shown in Figures 8 and 9. Both the ρ_{xy} section, identified as the electric field parallel-to-strike component, and the ρ_{yx} section, identified as the electric field perpendicular-to-strike component, show similar structure: (1) a continuous near-surface resistive layer, resistivities decreasing with depth and (2) an anomalously "conductive zone" at a depth of 400-500 m. These features are more regular in the ρ_{xy} component (Figure 8), which shows that the conductive layer thickness decreases with distance away from the summit while the layer resistivity increases from 2 to 10 ohm·m. A somewhat similar result appears in the ρ_{yx} results (Figure 9). We also used a two-dimensional inverse modeling scheme (Jupp and Vozoff, 1977) to fit the data. Although we did not obtain a satisfactory model fitting all the data, the shallower section was very similar to that obtained from the one-dimensional inversions.

Beneath the conductive zone (i.e., below a depth of ~1 km) the results show less continuity, except between Stations 2 and 2B, and it is difficult to draw conclusions regarding structure below -500 m in elevation. It has been

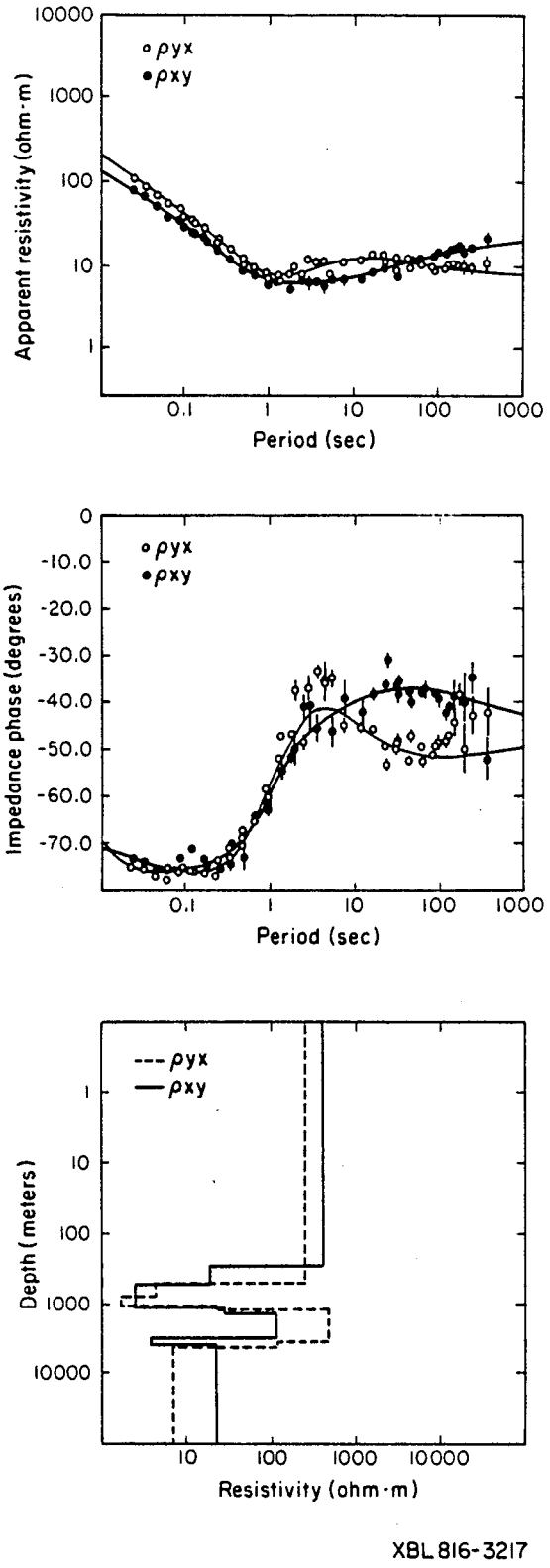

Figure 7. Apparent resistivity amplitude and phase spectra of the ρ_{xy} and ρ_{yx} components observed at Cloud Cap, Station 1. The layered-earth models are but two of many possible ones derived from an inversion of the amplitude and phase spectra.

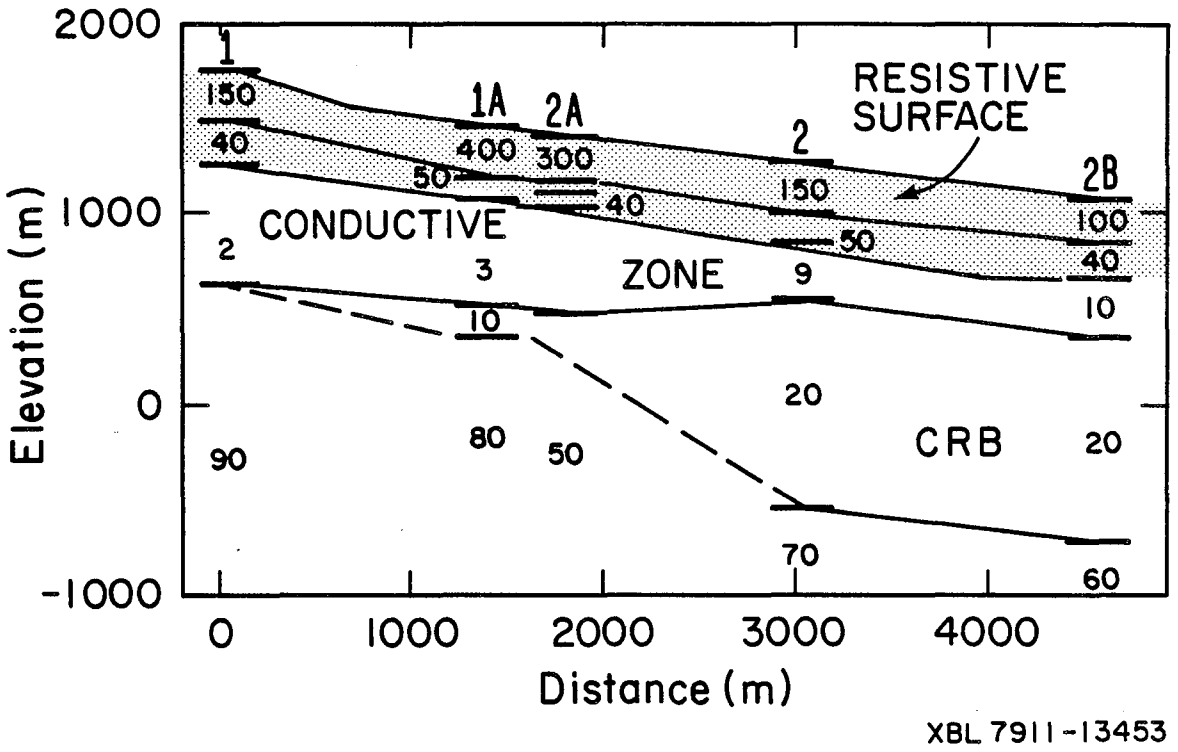

Figure 8. One-dimensional interpretation of the Cloud Cap line, electric field E-W (inferred electric field parallel-to-strike mode).

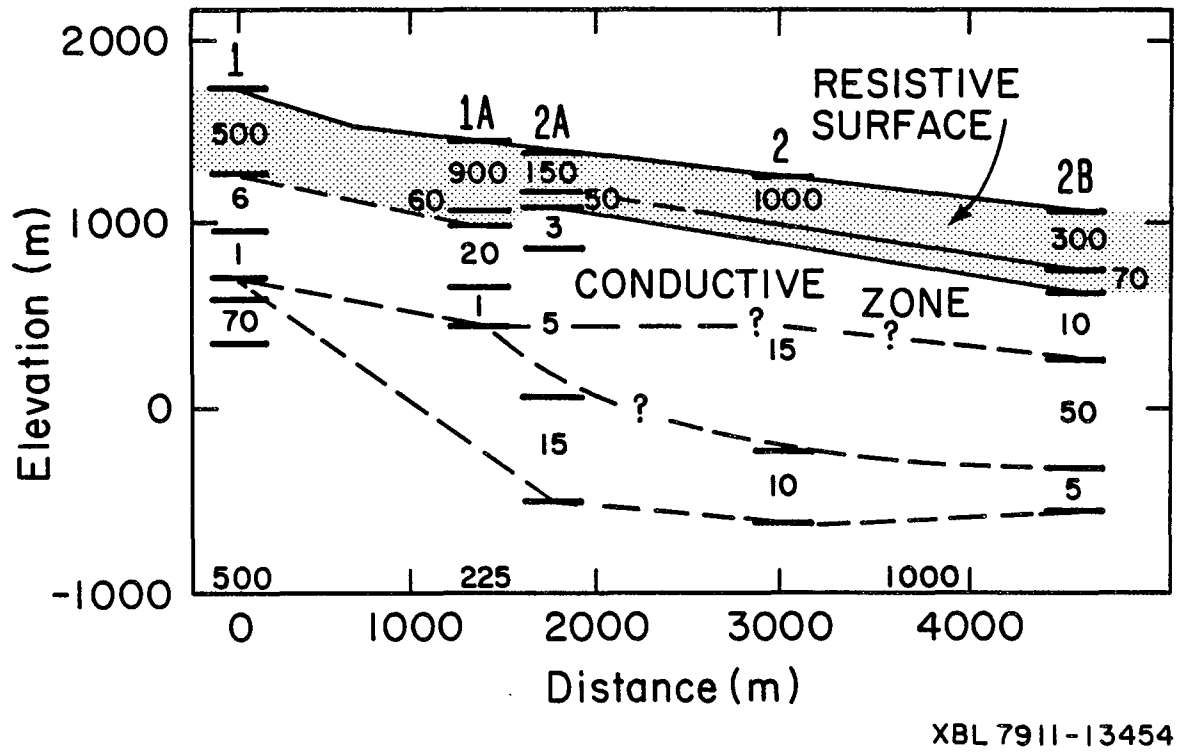

Figure 9. One-dimensional interpretation of the Cloud Cap line, electric field N-S (inferred electric field perpendicular-to-strike mode).

questioned whether the change in character of the impedance and tipper functions between Stations 1A/2A and 2 has actual geological significance or is merely a result of near-surface inhomogeneities. In an earlier report (Goldstein et al., 1979) we speculated that a concealed E-W to NE-SW fault occurs between those stations.

On the basis of geophysical and drill-hole data from the south flank (see next section), we have developed the following explanation for the shallow ($\leq$ 2 km) geophysical results consistent with water geochemistry (Wollenberg et al., 1979). The resistive surface layer is a partially saturated zone in which cold meteoric waters flow through porous pyroclastic and jointed volcanic flows. The anomalously low resistivity beneath this layer corresponds to saturated Mt. Hood volcanics containing warmer, possibly more saline, waters cooling progressively downslope as they mix with cold meteoric water. A possible heat source could be a still-hot Cloud Cap eruptive conduit or the main conduit beneath the summit.

The EM-60 sounding, for receiver CC 1 located 1 km from the transmitter loop, yielded data that were interpreted both through a joint inversion of the four amplitude and phase components and through an independent inversion of ellipticity only (Figures 10-12). Because of the small transmitter-receiver separation, the induced fields were unresponsive to the resistive zone below the conductive second layer; thus, only a two-layer earth is discerned. It may also be seen that ellipicity inversion seemed to define first-layer parameters better than amplitude and phase, although both approaches gave the same low probable error for the second-layer resistivity. These errors are estimates for a parametric representation of the earth, and are not accurate in terms of the real earth, which is considerably more complicated than our

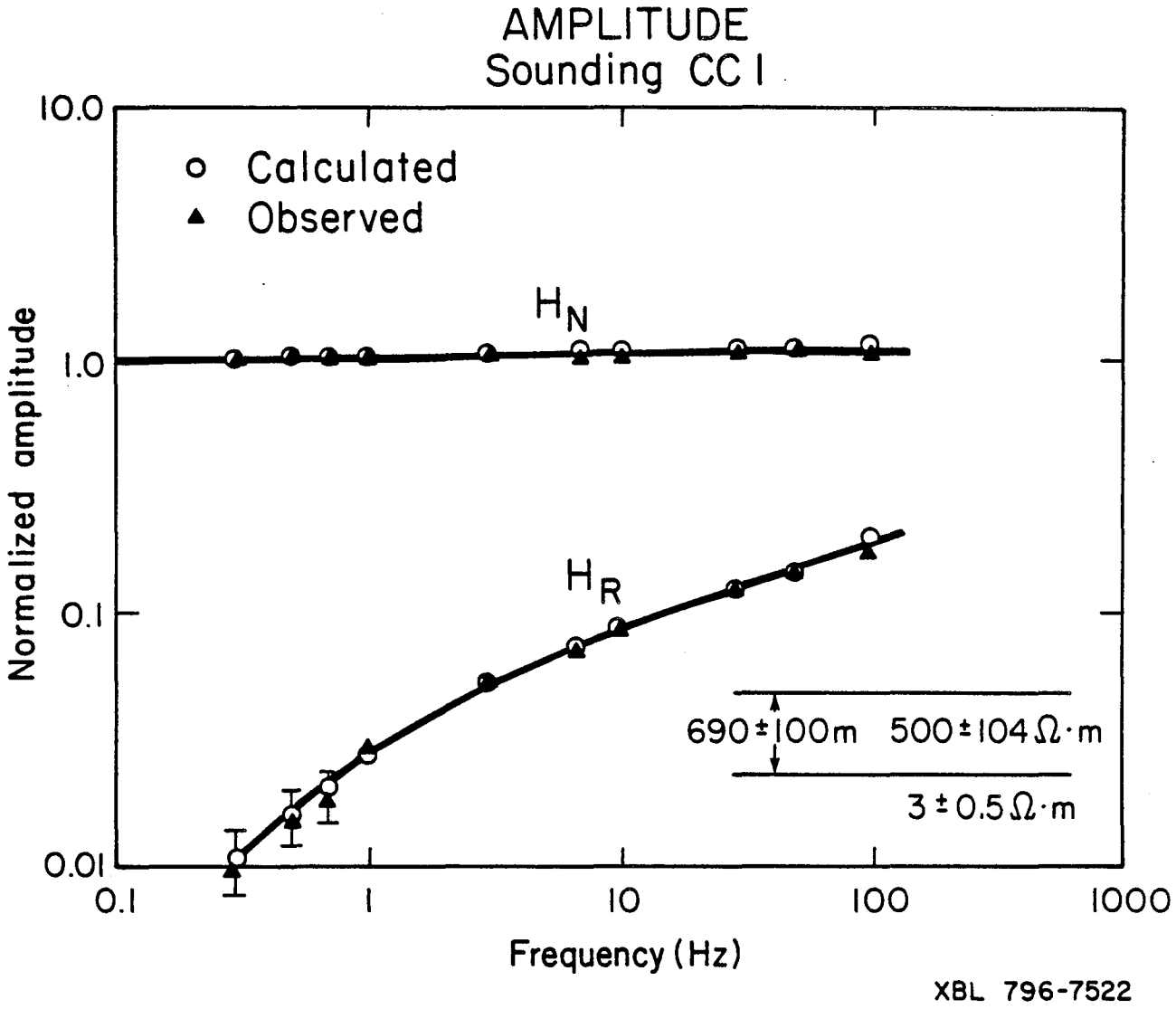

Figure 10. Amplitude spectra of vertical (H_N) and radial (H_R) components at receiver station CC1 relative to the Cloud Cap EM-60 transmitter loop.

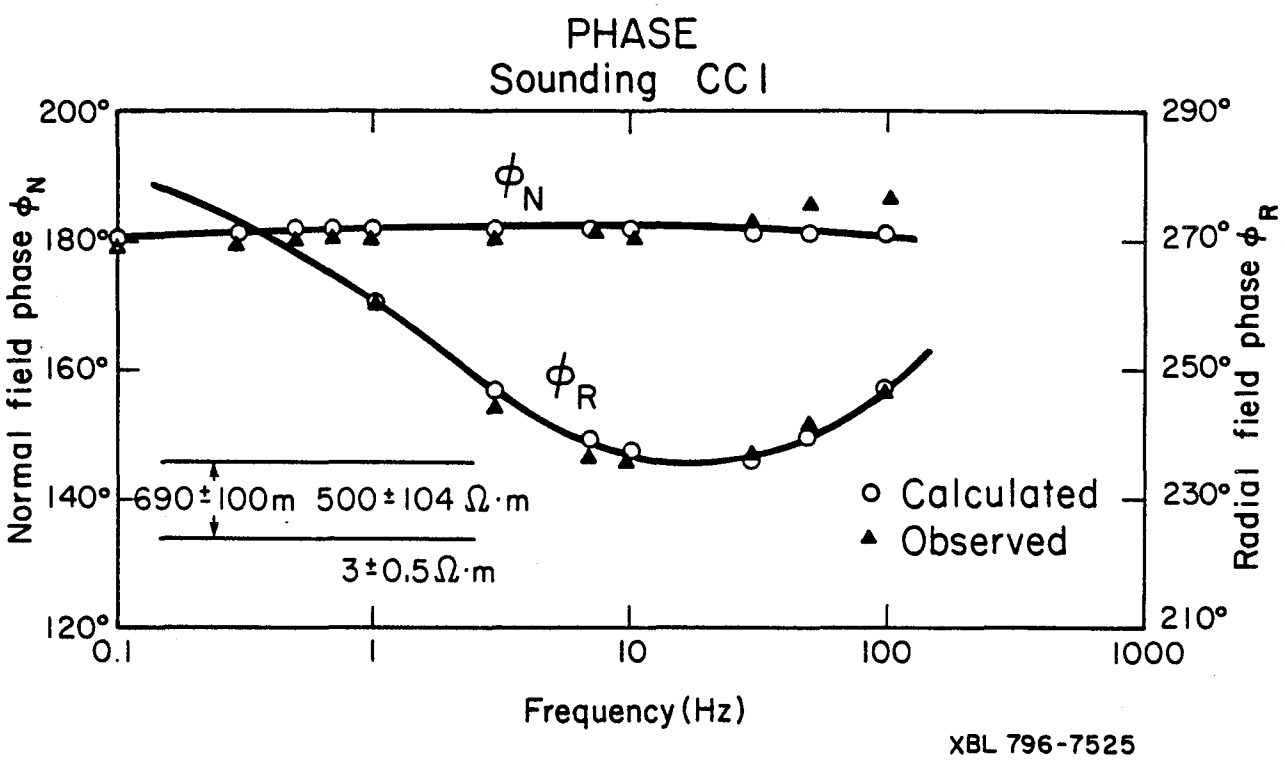

Figure 11. Phase spectra of vertical (ϕ_N) and radial (ϕ_R) components for station CC1 (see Figure 11).

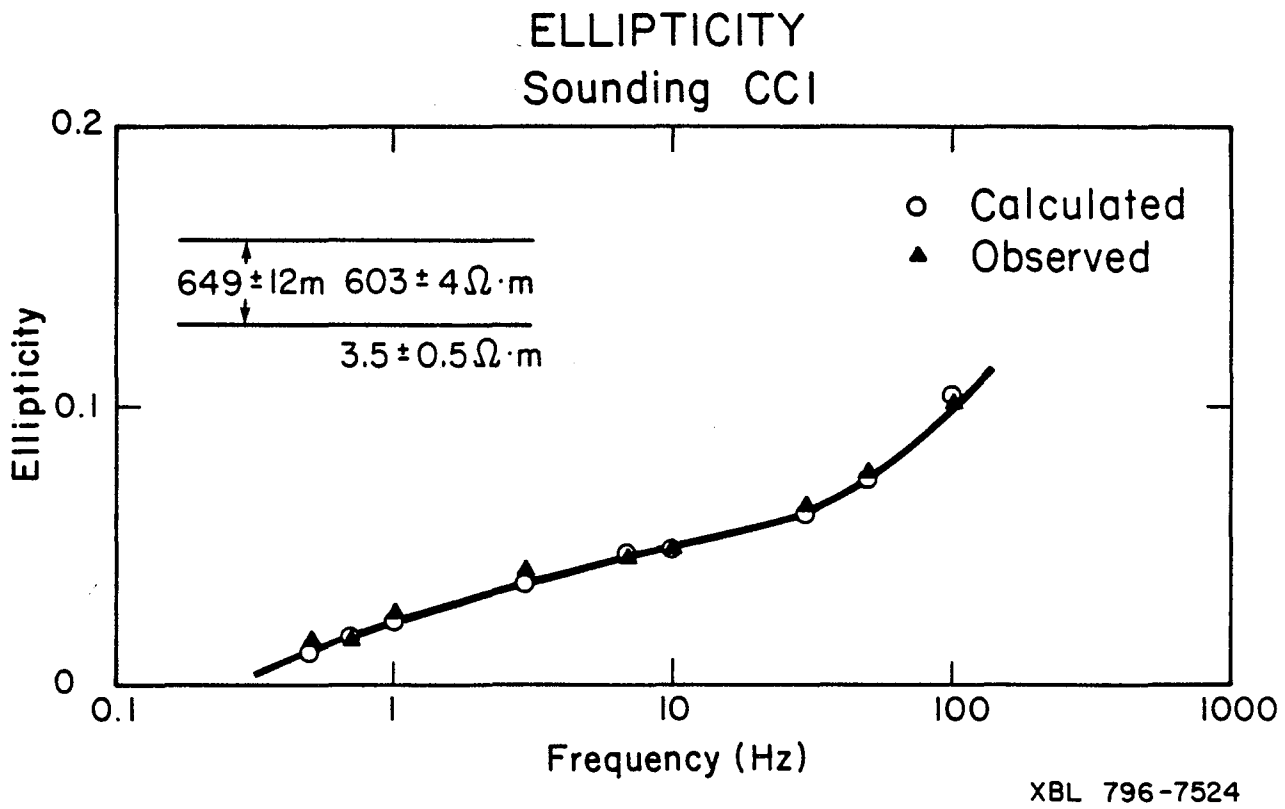

Figure 12. Ellipticity spectrum for Station CC1 (see Figure 11).

simple model of two layers and three parameters. The probable errors are geologically significant only to the extent that they indicate how closely we can fit the observed data to a simple layered model. The EM-60 sounding for receiver Station CC 2 could not be fitted with low error to a layered earth, possibly because of severe local relief between transmitter and receiver.

In general, EM sounding interpretations for Station CC 1 are similar to the near-surface portion of the MT interpretations. The most obvious difference between the two is in the thickness of the resistive surface layer. This difference was noted at other sites at Mt. Hood, and will be discussed in the next section.

Timberline Lodge

Timberline Lodge is located at the 1820-m elevation on the relatively gently sloping south flank of Mt. Hood. Because of continuing efforts by the lodge operator to find a source of hot water to heat the main lodge and a new day lodge, several MT and EM soundings were made in the area. An EM transmitter loop was laid out a short distance east of the main lodge, and four receiver stations were occupied at distances of 1-2 km from the transmitter. The most distant receiver (TL 2) was located at the top of the Miracle Mile chair lift (2425-m elevation), approximately 2 km north of Timberline Lodge. This was our closest approach to the summit.

Several MT soundings were attempted in the area, but, because of noise, only Station 13 provided enough data for an interpretation. However, this MT station and EM receiver station TL 4 are close to a geothermal test well later drilled at the base of the Pucci chair lift, 1 km south of the lodge.

Figure 13 shows the MT sounding results from Station 13. The strong separation between apparent resistivities in the principal directions is an indication of two- and three-dimensional structures. Despite reference magnetic reprocessing, ρ_{xy} apparent resistivity values remain badly scattered in the range of 1-10 sec, although the error statistics are immensely improved over the initial results. Because the electric field was strongly polarized in the area, we were unable to define a ρ_{yx} apparent resistivity sounding curve without large error. Consequently, the ρ_{yx} curve is drawn as a dashed line to indicate its approximate configuration.

Cognizant of the pitfalls of accepting a one-dimensional interpretation, we nevertheless show for the sake of comparison and discussion one such partial interpretation in Figure 13. Here, the same general near-surface layering is found as at Cloud Cap--a resistive surface layer, resistivity poorly resolved, underlain at a depth of approximately 350 m by a thin conductive zone. Of the many inversions made with constrained and unconstrained parameters, the one shown in Figure 13 for a joint inversion of apparent resistivity amplitudes and phases with no constraints yielded a fit as good as or better than others. The absence of high frequency data points impairs our ability to resolve the resistivity of the surface layer, but this does not interfere with our resolution of the 3 ohm·m second layer. Parameters derived for the third and fourth layers are probably in error, and no geological inferences should be drawn from them. In this regard, one should note the phase behavior at periods longer than, say, 30 sec. The phase curves, as well as those shown in Figures 22 and 23, cannot be matched by any one-dimensional model, indicating that the deeper structure requires a multi-dimensional model.

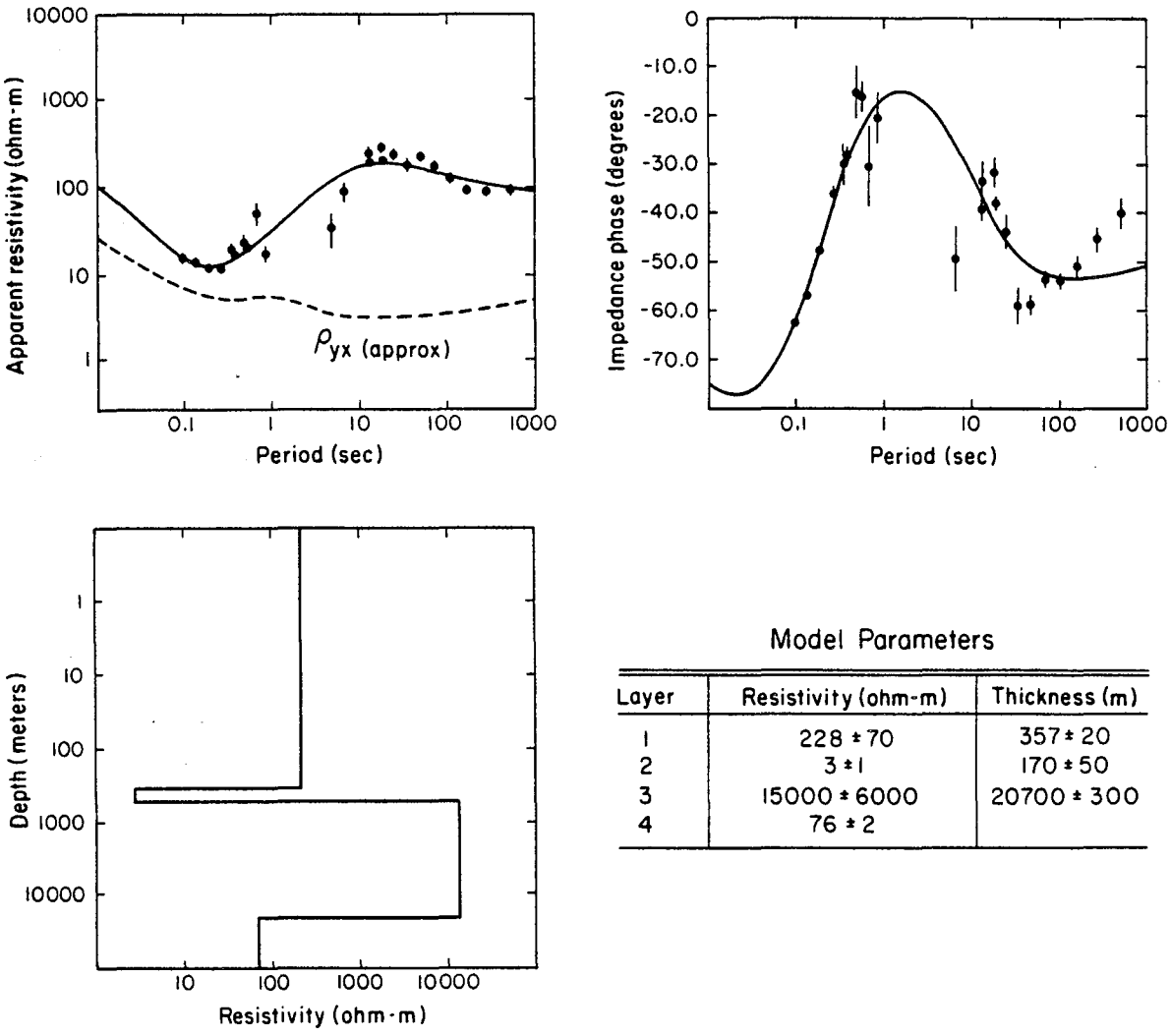

Model Parameters

Layer	Resistivity (ohm-m)	Thickness (m)
1	228 ± 70	357 ± 20
2	3 ± 1	170 ± 50
3	15000 ± 6000	20700 ± 300
4	76 ± 2	

Figure 13. MT sounding curves for Station 13 (Timberline Lodge) and the 1-D interpretation of the TE mode curve.

Controlled-source EM sounding results relative to receivers located 1 km north and 1 km south of the Timberline transmitter (soundings TL 3 and TL 4, respectively) are shown in Figures 14-19. Since the results are not particularly sensitive to first-layer resistivity, we have constrained this parameter to 500 $\Omega \cdot m$ in the amplitude-phase inversion. Results show a layering similar to that found at the same elevation on the northeast flank (Cloud Cap). They also verify that the MT second-layer conductor is real and not an artifact of applying a 1-D inversion to 2-D and 3-D data. In contrast to the Cloud Cap area, it appears that the Timberline area has a thinner first layer and a less conductive second layer.

Comparing the Timberline MT and EM results, we see differences in the subsurface models that require some discussion and explanation. One notable difference is that the EM discerns a deeper and less conductive second layer. When the EM subsurface model is used in an MT forward calculation, the resulting curves differ significantly from those in Figure 13. While there may be several reasons for the differences in the models, one is that a 1-D inversion of MT data taken in complex areas is more susceptible to error than the 1-D inversion of the corresponding EM sounding because of the more focused nature of the dipole field. For example, we show in Figure 20 the error in the estimated depth to an embedded 2-D conductor that results when we apply a 1-D MT inversion. Curves $E_{\parallel}$ and $E_{\perp}$ are the calculated sounding curves for E-field parallel-to-strike and perpendicular-to-strike, respectively. Performing the conventional 1-D inversion on $E_{\parallel}$ results in a three-layer model that fits the data very well. However, the conductor depth is underestimated by 34% in this example.

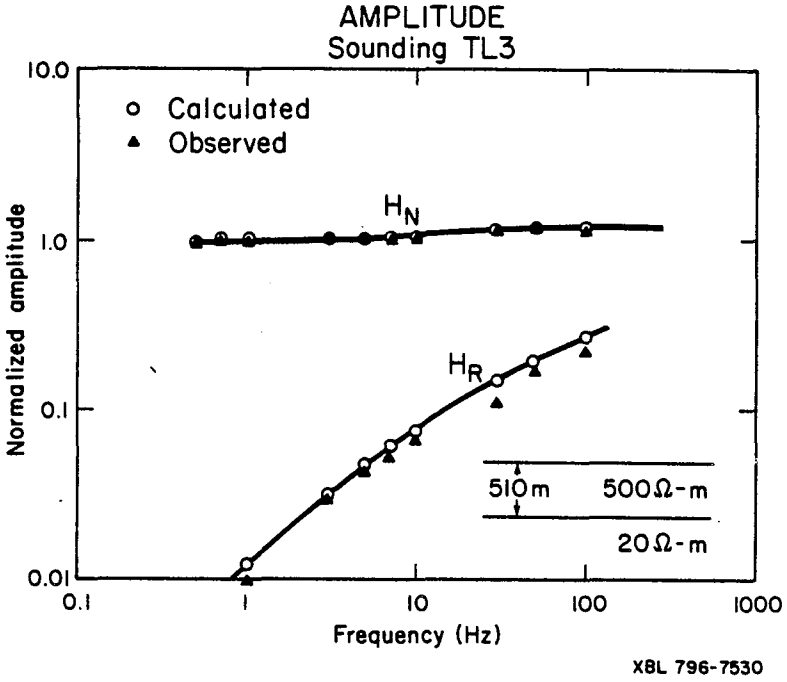

Figure 14. Amplitude spectra of vertical (H_N) and radial (H_R) components at receiver station TL3 relative to the Timberline Lodge EM-60 transmitter.

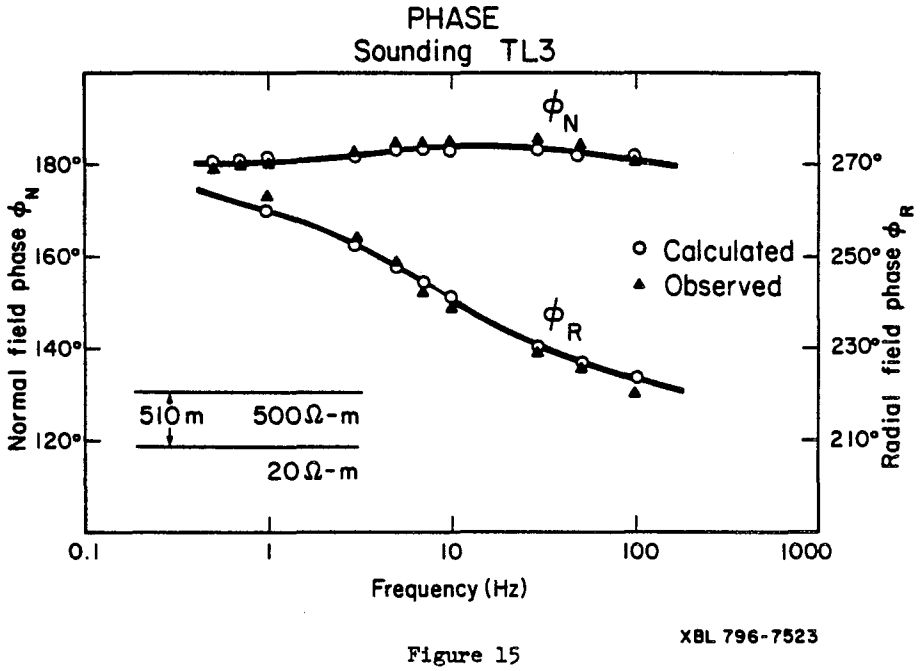

Figure 15

Figure 15. Phase spectra of vertical (ϕ_N) and radial (ϕ_R) components for station TL3.

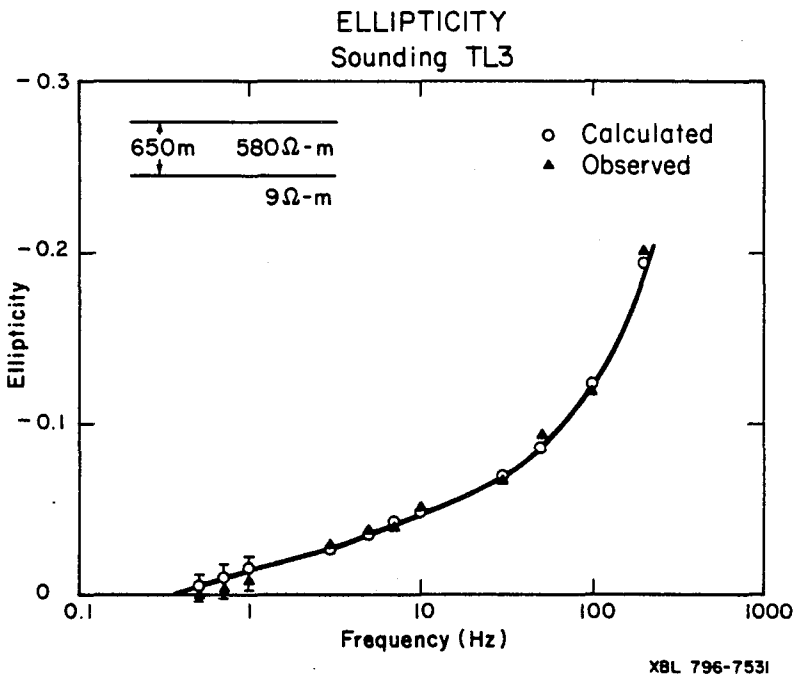

Figure 16. Ellipticity spectrum for Station TL3.

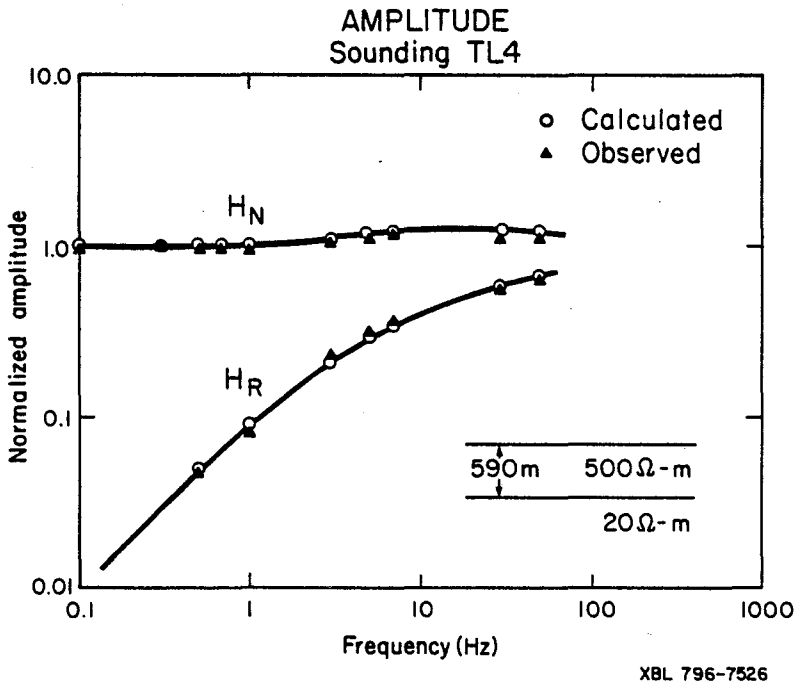

Figure 17. Amplitude spectra of vertical (H_N) and radial (H_R) components at receiver station TL4 relative to the Timberline Lodge EM-60 transmitter.

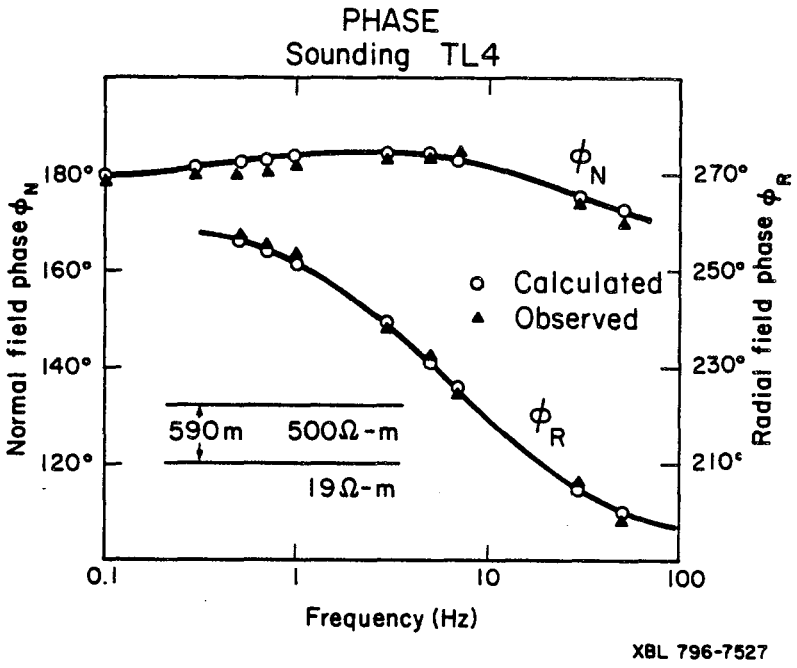

Figure 18. Phase spectra of vertical (ϕ_N) and radial (ϕ_R) components for station TL4.

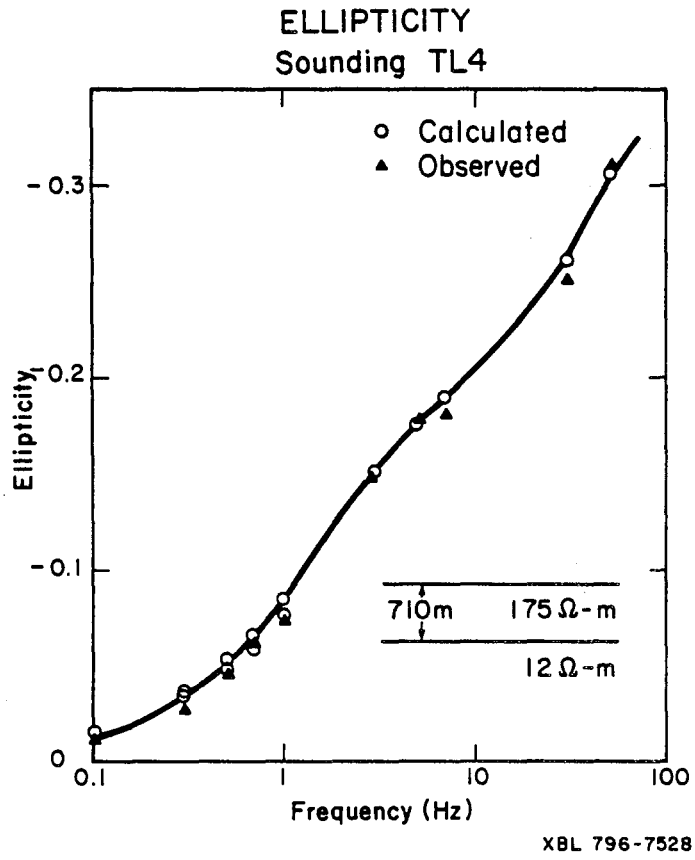

Figure 19. Ellipticity spectrum for station TL4.

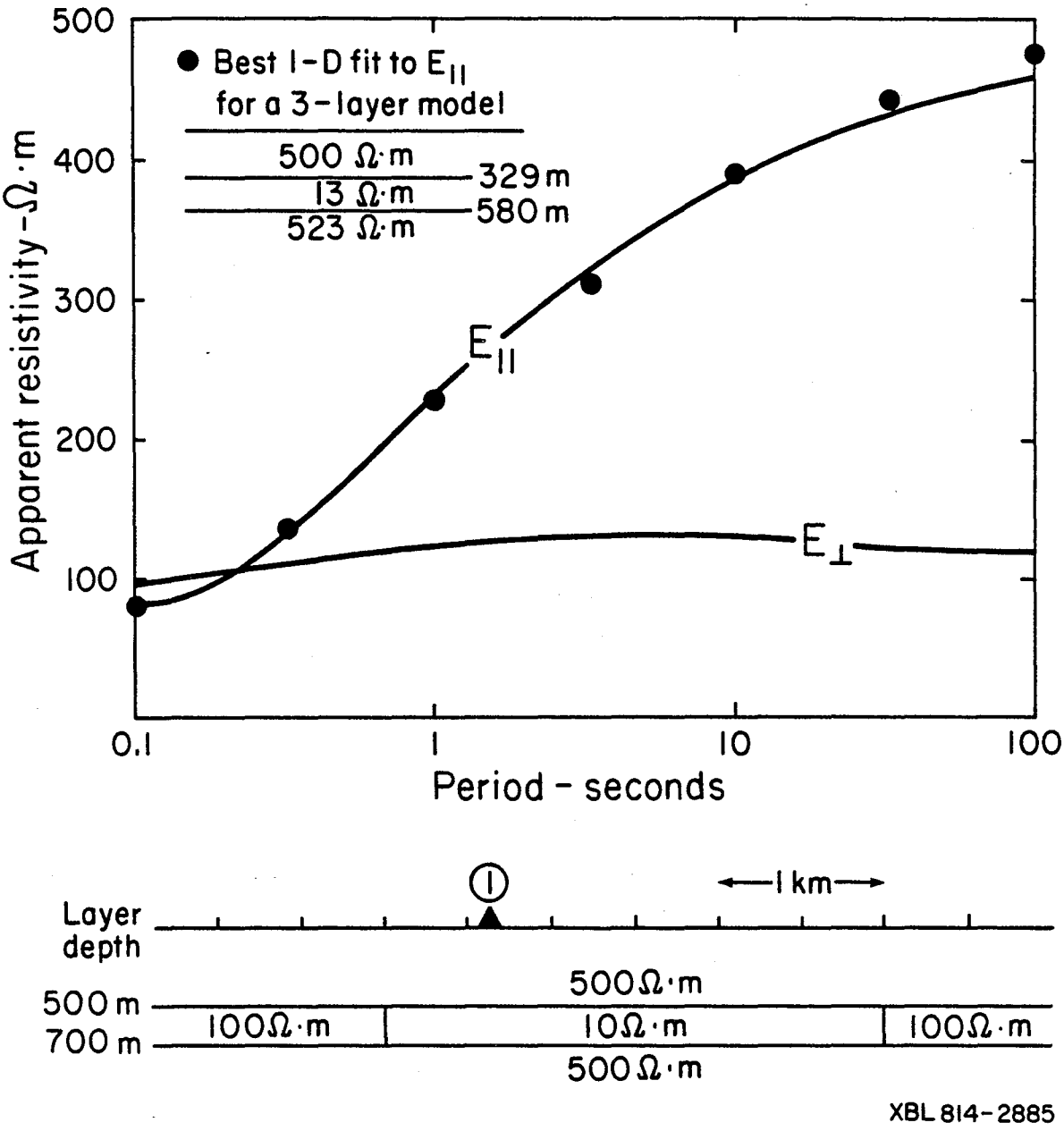

Figure 20. Underestimation of depth to an embedded 2-D conductor using a 1-D inversion of the E-field parallel-to-strike ($E_{\parallel}$) component at Station 1.

In the actual field case, the better accuracy of a 1-D inversion of the EM data seems to be verified by drill-hole results. In 1980, the Pucci geothermal test hole (35/9E-7db) was drilled to a depth of 1213 m by the U.S. Geological Survey and DOE. The hole is located near MT Station 13 and EM receiver station TL 4. Two weeks after drilling, the water level was 570 m below the surface, at which depth the temperatures were in the 40-50°C range and the bottom-hole temperature appeared to be equilibrating at 70-80°C (J. Robinson, 1981, personal communication). Because the top of the saturated zone conforms so closely to the interpreted EM conductor at 590 m (Figures 17 and 18), we feel reasonably confident that the second-layer conductor represents the saturated zone. The fact that the second layer underlying the Cloud Cap area is 5 to 10 times more conductive than at Timberline Lodge may indicate that higher temperatures exist on the northeast flank of the volcano.

Summit Meadows

Summit Meadows (elevation 1106 m) lies approximately 10.5 km south of the summit and 1.5 km south of the Still Creek Campground, site of the warm waters known collectively as Swim Warm Springs. Because of this geothermal evidence, a number of MT stations and one EM-60 transmitter with three receiver sites were occupied in the NNE-trending valley between Trillium Lake and Highway 26.

Three EM receivers were located north, west, and south of a transmitter loop laid out in Summit Meadows, but only the data from Station SM 1, located 1.3 km north of the loop, are subject to simple interpretation (Figure 21). Although we obtain roughly the same type of resistivity section as higher on the flanks of the volcano, the surface layer is much less resistive in the meadows. The nearest MT station yielding good data is Station 11 (Figure 22), and a one-dimensional inversion was made on the ρ_{xy} component. In this

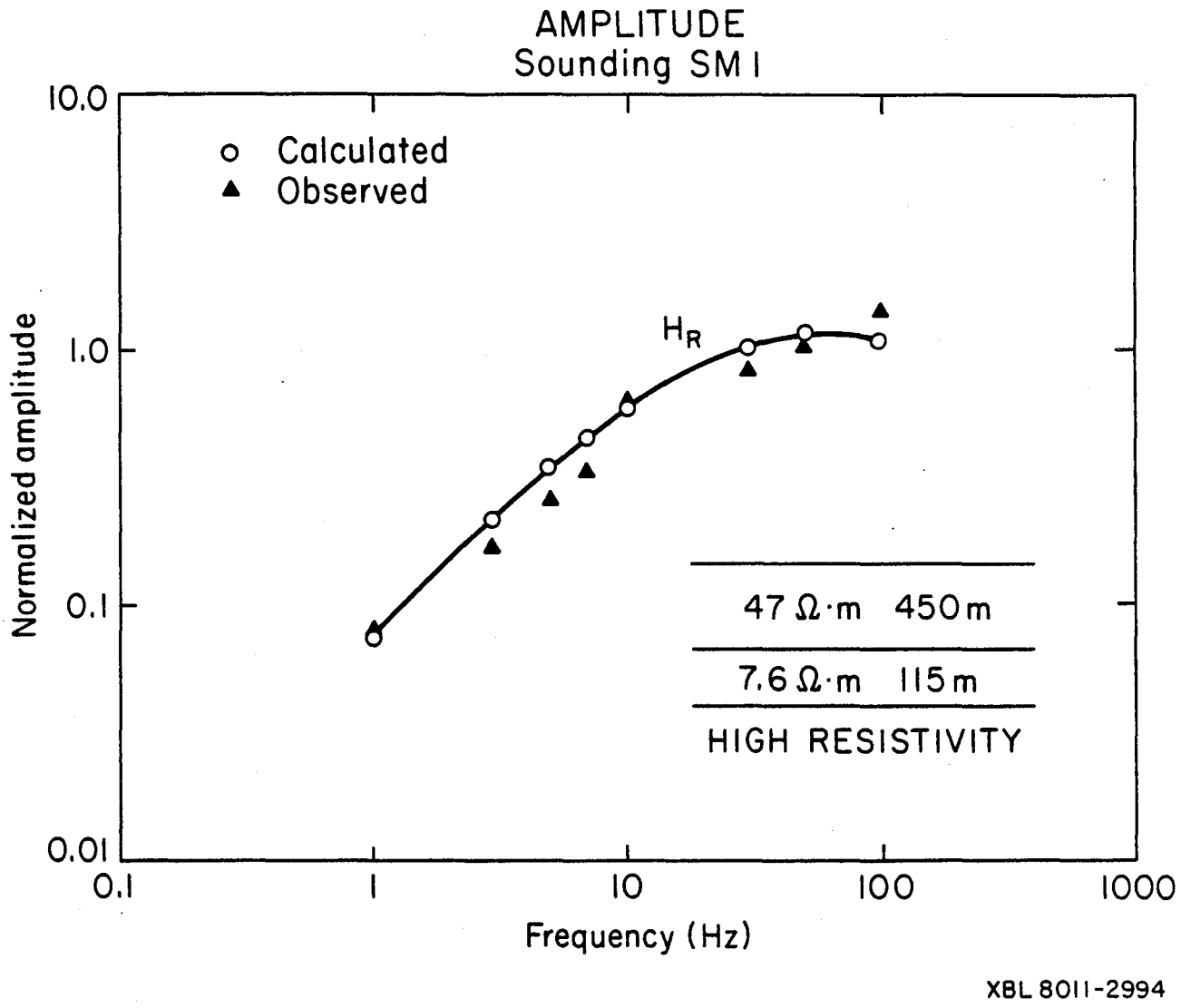

Figure 21. Amplitude spectrum of the radial component (H_R) for Station SM1 in Summit Meadows.

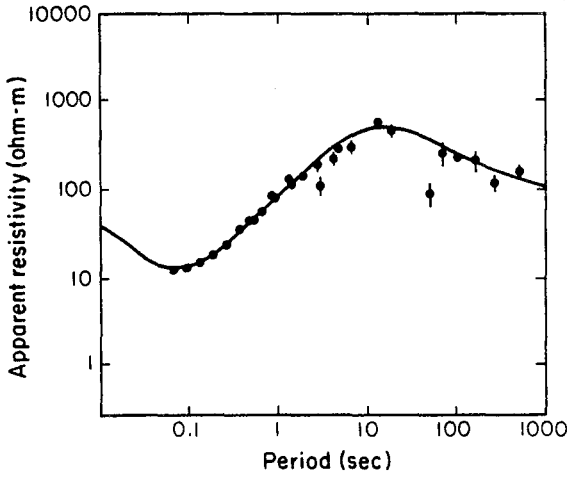

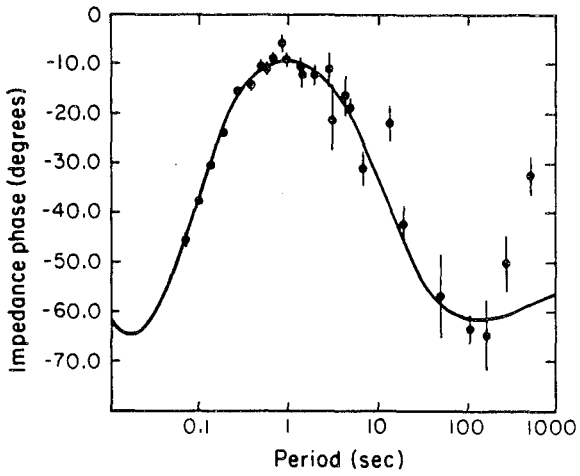

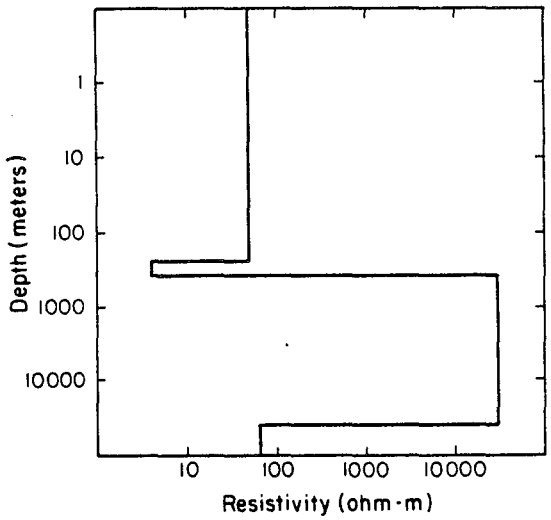

Model Parameters

Layer	Resistivity (ohm-m)	Thickness (m)
1	50 ± 0	230 ± 20
2	4 ± 1.5	140 ± 40
3	32300 ± 14000	38200 ± 400
4	70 ± 1.5	

XBL 811-2513

Figure 22. MT sounding curves at Station 11, Summit Meadows, and the one-dimensional interpretation based on the TE mode.

inversion we imposed a 50 ohm·m constraint on the surface layer, as dictated by the EM results, and obtained a good fit to amplitude and phase data points. As at other stations, the MT gives a thinner first layer than the EM, but second layer resistivities agree fairly well. Data from MT Station 14, located 1 km east of Station 11 on pre-Mt. Hood volcanics, were interpreted on the basis of various constraints, including no constraints on layer parameters (Figure 23). At this site the conductive second layer is discerned at the same shallow depth, but now appears as a thinner, more conductive zone.

Old Maid Flat

A cluster of one MT and three remote telluric MT stations were occupied in the Old Maid Flat area, 13.5 km west of the summit. This was the point closest to the road approach on the west flank and near the sites of the Old Maid Flat (OMF) #1 and OMF #7A geothermal wells drilled by Northwest Natural Gas and DOE to depths of approximately 1200 m and 1838 m, respectively. Bottom-hole temperatures were 82° and 112°C, respectively, but both holes are essentially dry at depth (John Hook, 1981, personal communication).

Hood River

Two MT and four remote telluric stations were occupied in an approximate east-west line extending from Lookout Mountain on the east across the East Fork of the Hood River to the Hood River Meadows, a distance of 8 km. These stations were surveyed to determine whether MT could discern the postulated north-south normal fault following the river and the graben-like structure related to crustal swelling and subsidence west of the river. A gradient hole was drilled to 352 m at Mt. Hood Meadows (35/9E-3cca) by the U.S. Geological Survey and DOE in 1980. The bottom-hole temperature was only 12°C, but the thermal gradient was 75°C/km in the lower part of the hole beneath

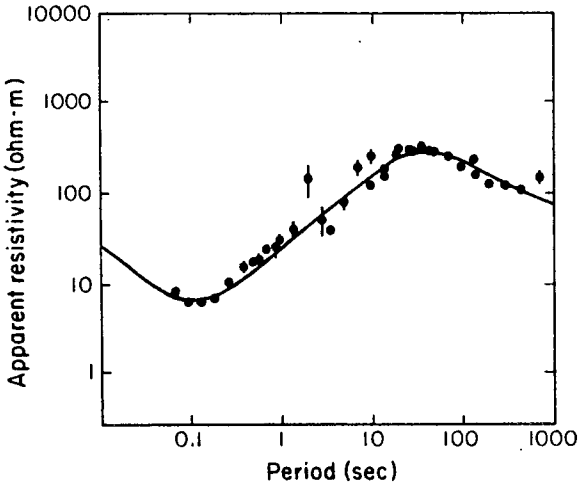

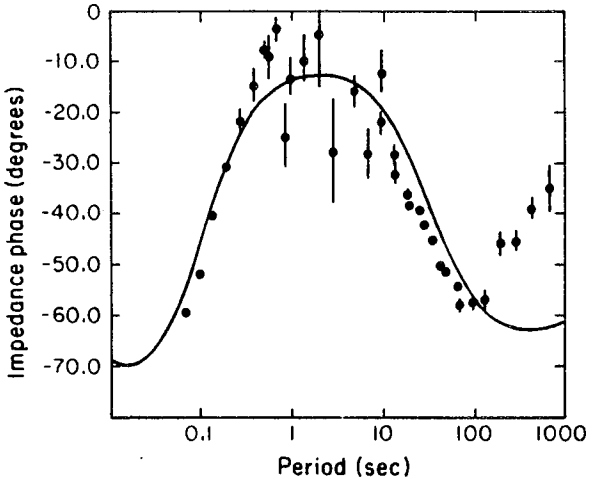

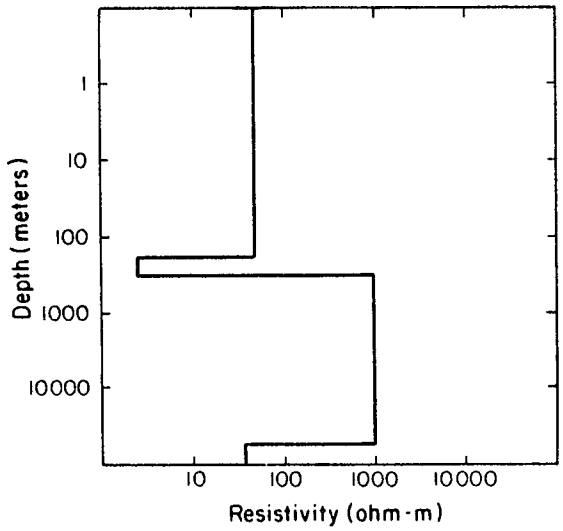

Model Parameters

Layer	Resistivity (ohm-m)	Thickness (m)
1	50 ± 0	179 ± 30
2	2.5 ± 1.5	133 ± 60
3	1054 ± 56	53500 ± 1300
4	38 ± 3.0	

XBL 811-2553

Figure 23. MT sounding curves at Station 14, Summit Meadows, and the one-dimensional interpretation based on the TE mode.

a cold isothermal zone (J. Robinson, 1981, personal communication).

White River

Two MT and three remote telluric stations were occupied along an approximate north-south line in the White River area. These stations were surveyed to obtain more complete coverage on the south flank of the volcano.

REPRESENTATION OF MAGNETOTELLURIC RESULTS OVER THE SURVEY AREA

As a first step toward analyzing the lateral conductivity variations over an area, selected magnetotelluric parameters may be plotted in polar diagram form (Reddy et al., 1977). This procedure compresses and simplifies a great deal of information, thus allowing us to gain some geological insights as to local and regional structure. In this report, we show polar diagrams for both apparent resistivity (ρ_{xy}) and tipper magnitude (T_y). Figures 24-26 show these polar plots at each station for three bands--a high-frequency band between 10 and 40 Hz, a midband between 0.1 and 1.0 Hz, and a low-frequency band below 0.01 Hz.

The function ρ_{xy} (ϕ,ω), where ϕ is the azimuthal angle from north, was calculated from the off-diagonal term $Z_{xy}(\omega)$ of the impedance tensor. First, an analytical rotation of the $Z_{xy}(\omega)$ was performed over 360 degrees, and these values were then averaged within selected frequency bands.

The size of the polar diagram is logarithmically related to apparent resistivity, and the maximum-minimum axes reveal the principal resistivity directions. A circular diagram is indicative of layered earth conditions, whereas a diagram constricted in one direction into a "peanut" or "figure 8"

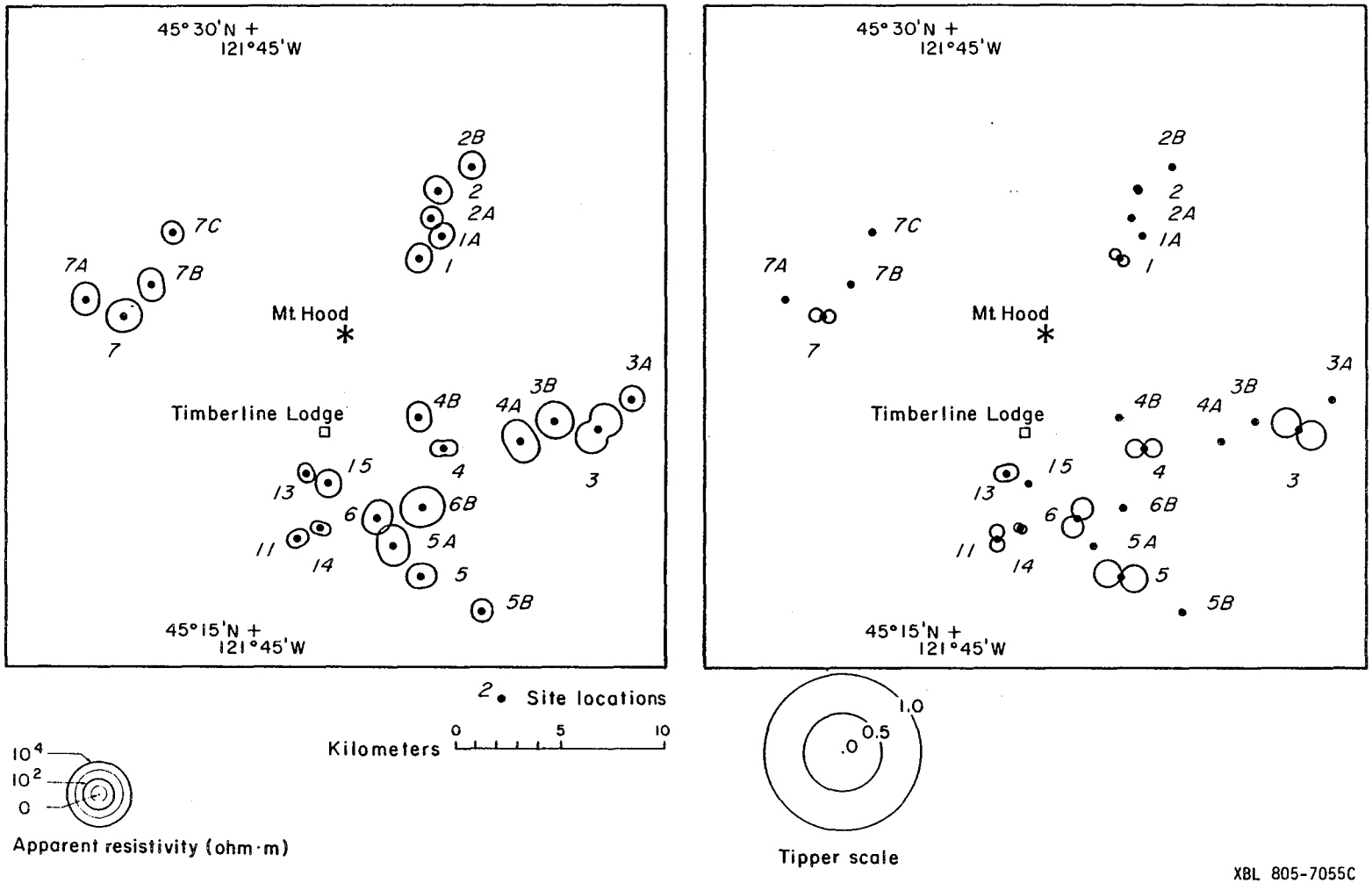

Figure 24. Apparent resistivity and tipper polar diagrams, ρ_{xy} and T_y, averaged in the band above 10 Hz.

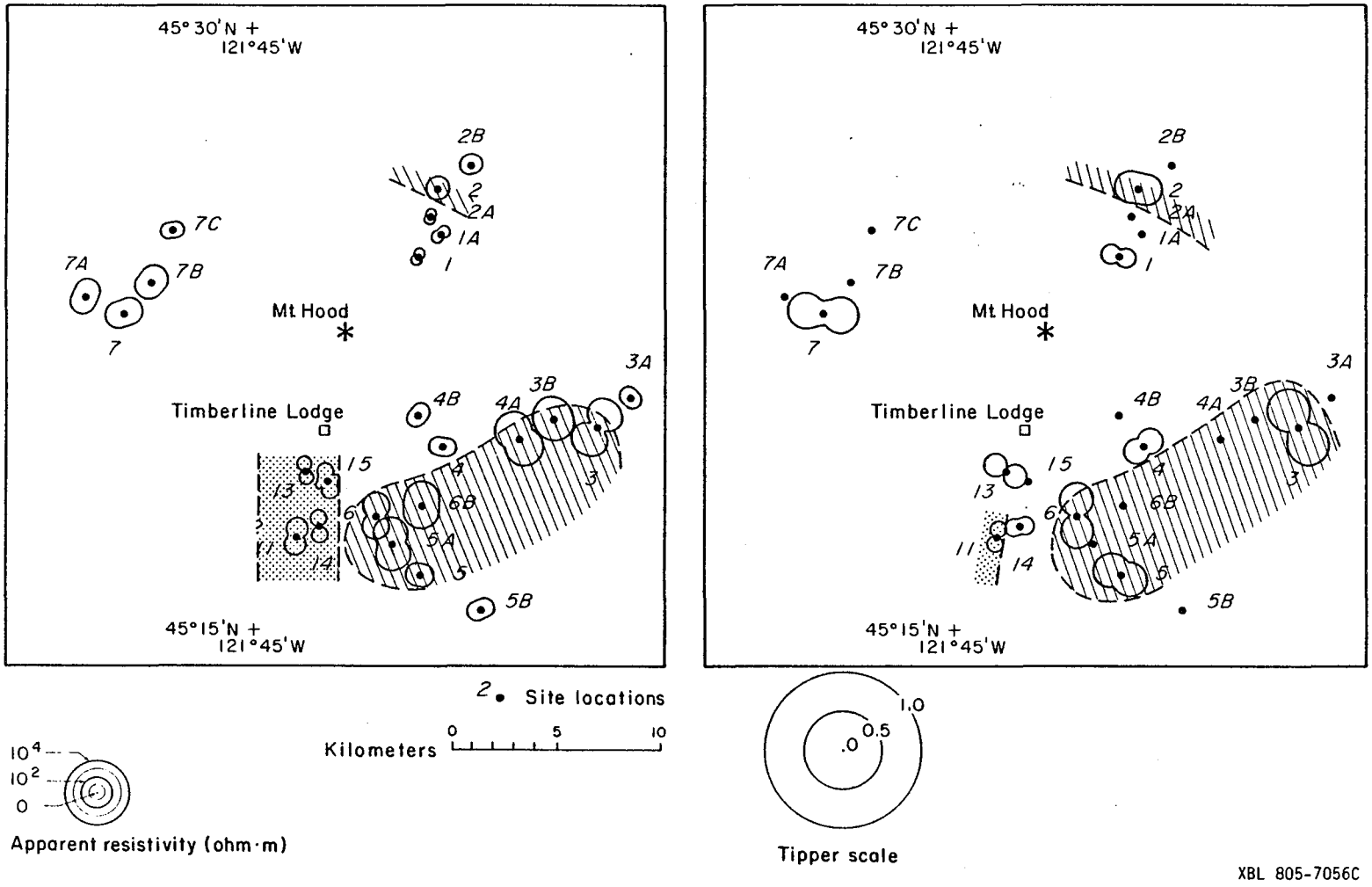

Figure 25. Apparent resistivity and tipper polar diagrams, ρ_{xy} and T_y, averaged in the 0.1 to 1.0 Hz bands. The shaded areas are resistive zones, the stippled areas are conductors.

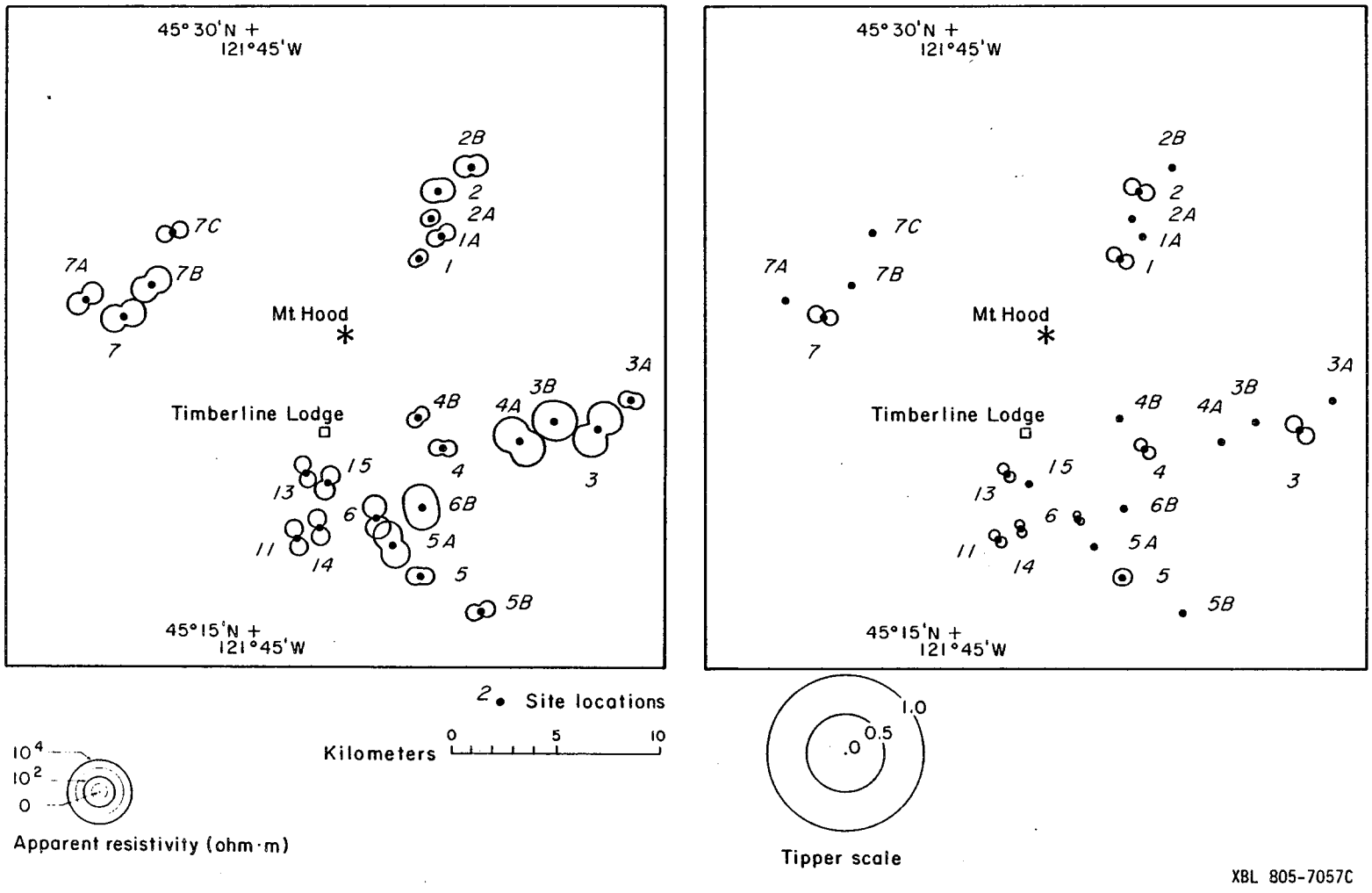

Figure 26. Apparent resistivity and tipper polar diagrams, ρ_{xy} and T_y, averaged in the band below 0.01 Hz.

shape suggests resistivity anisotropy and current channeling in preferrred directions. The high-frequency diagrams show the least nonuniformity, and the low-frequency diagrams show the greatest--indicating increasing structural complexity with depth. Several areas stand out as anomalous: (1) the low-resistivity zone previously discussed in reference to Cloud Cap; (2) a low-resistivity zone south of Timberline Lodge in the Summit Meadows-Swim Warm Springs area, where we see evidence for a north-south conductivity anomaly; and (3) the generally high resistivities and variable principal directions at Stations 3 and 4, which span the Hood River (the river passes through Station 3B). These plots also illustrate the horizontal distances over which large-scale resistivity changes occur.

On the scale of station clusters (~ 5 km), amplitudes and directions may remain fairly consistent (as at clusters 1 and 2, Cloud Cap) or change markedly by orders of magnitude and 90 degrees over short distances, such as within cluster 3 (Hood River) and on the south side of the mountain (White River-Bennett Pass). A combination of local topography and geology seems to be the cause for the intracluster variability in several areas. For example, with the exception of the easternmost Station 3C in cluster 3, the high apparent resistivities at all frequencies seem to be related to the older, pre-Mt. Hood (Pliocene) volcanics at or near the surface east and west of the Hood River. Station 3C sits on Holocene basalt-andesite, close to the vent of an eruption of the same type and age as Cloud Cap. The Station 3C apparent resistivity polar diagrams show higher conductivities and other characteristics similar to those at the Cloud Cap stations.

Complementary to the ρ_{xy} polar diagrams, we also show the corresponding tipper diagrams. These diagrams relate the amplitude ratio between the vertical and horizontal magnetic fields for a 360-degree rotation of the

REFERENCES

Allen, J.E., The Cascade Range volcano-tectonic depression in Oregon, in Trans. Lunar Geol. Field Conf., Department of Geology and Mineral Industries, State of Oregon, Bend, Oregon, August 1965, p. 21-23, 1966.

Bacon, C.R., Geology and geophysics of the Cascade Range, Abs. 51st Annual International Meeting Soc. Expl. Geophysicists, Tulsa, Oklahoma, 1981.

Beeson, M.H., and Moran, M.R., Stratigraphy and structure of the Columbia River basalt group in the Cascade Range, Oregon, in Geothermal Resources Assessment of Mt. Hood, Final Report, Department of Geology and Mineral Industries, State of Oregon, p. 5-77, 1979.

Callaghan, E., Some features of the volcanic sequence in the Cascade Range in Oregon, Trans., Am. Geophys. Un., p. 243-249, 1933.

Couch, R. and Gemperle, M., Gravity measurements in the area of Mt. Hood, Oregon, in Geothermal Resources Assessment of Mount Hood, Final Report, Department of Geology and Mineral Industries, State of Oregon, p. 137-187, 1979.

Crandell, D.R., Recent eruptive history of Mount Hood, Oregon, and potential hazards from future eruptions, U.S. Geol. Survey Bull. 1492, 1980.

Crandell, D.R., and Rubin, M., Late glacial and post-glacial eruptions at Mt. Hood, Oregon, Geol. Soc. Am., Abs. with Prog., 9 (4), p. 406, 1977.

Folsom, M.M., Volcanic eruptions: The pioneers' attitudes on the Pacific Coast from 1800 to 1875, Ore Bin, 32 (4), p.61-71, 1970.

Gamble, F.D., Goubau, W.M., and Clarke, J., Magnetotellurics with a remote reference, Geophysics, 44, p. 53-68, 1979.

Goldstein, N.E., and Mozley, E., A telluric-magnetotelluric survey at Mt.Hood, Oregon--A preliminary study, Lawrence Berkeley Laboratory, Berkeley, Calif., LBL-7050, 1978.

Goldstein, N.E., Mozley, E., Gamble, T.D., and Morrison, H.F., Magnetotelluric investigations at Mt. Hood, Oregon, Geoth. Res. Council, Trans. 2, p. 219-221, 1978.

Goldstein, N.E., Wilt, M., Stark, M., Mozley, E. and Morrison, H.F., Magnetotelluric and controlled-source electromagnetic studies at Mt. Hood, Oregon, Lawrence Berkeley Laboratory, Berkeley, Calif., LBL-9776, 1979.

Hermance, J.F., and Thayer, R.E., The telluric-magnetotelluric method, Geophysics, 40, p. 664-668, 1976.

Inman, J.R., Resistivity inversion with ridge regression, Geophysics, 38, p. 798-817, 1975.

Jupp, D.L.B., and Vozoff, K., Stable iterative methods for the inversion of geophysical data, Geophys. J., Royal Astr. Soc., 42, p. 957-976, 1975.

Jupp, D.L.B., and Vozoff, K., Two-dimensional magnetotelluric inversion, Geophys. J., Royal Astr. Soc., 50, p. 333-352, 1977.

Law, L.K., Auld, D.R., and Booker, J.R., A geomagnetic variation anomaly coincident with the Cascade Volcanic Belt, J. Geophys. Res., 85, p. 5297-5302, 1980.

Morrison, H.F., Goldstein, N.E., Hoversten, M., Oppliger, G., and Riveros, C., Description, field test and data analysis of a controlled-source EM system (EM-60), Lawrence Berkeley Laboratory, Berkeley, Calif., LBL-7088, 1978.

Reddy, I.K., Rankin, D., and Phillips, R.J., Three-dimensional modeling in magnetotelluric and magnetic variational sounding, Geophys. J., Royal Astr. Soc., 51, p. 313-325, 1977.

Stanley, W.D., A regional magnetotelluric survey of the Cascade Mountain region, U.S. Geol. Surv. Open File Rep., Denver, 1980.

Thayer, T.P., Petrology of the later Tertiary and Quaternary rocks of the north-central Cascade Mountains in Oregon, with notes on similar rocks in Nevada, Geol. Soc. Am. Bull., 48, 1611-1652, 1937.

White, C.M., Geology and geochemistry of Mt. Hood, Oregon, in Geothermal Resources Assessment of Mt. Hood, Final Report, Department of Geology and Mineral Industries, State of Oregon, 78-136, 1979.

Wilt, M., Goldstein, N.E., Hoversten, M., and Morrison, H.F., Controlled-source EM experiment at Mt. Hood, Oregon, Geothermal Resources Council, Trans., 3, p. 789-792, 1979.

Wise, W.S., Mount Hood area, in Andesite Conf. Guidebk., Oregon Department of Geology and Mineral Industries, Bull. 62, p. 81-98, 1968.

Wollenberg, H.A., Bowen, R.E., Bowman, A.R., and Strisower, B., Geochemical studies of rocks, water, and gases at Mt. Hood, Oregon, Lawrence Berkeley Laboratory, Berkeley, Calif., LBL-7092, 1979.

This report was done with support from the United States Energy Research and Development Administration. Any conclusions or opinions expressed in this report represent solely those of the author(s) and not necessarily those of The Regents of the University of California, the Lawrence Berkeley Laboratory or the United States Energy Research and Development Administration.